Electronic Research Archive

https://www.aimspress.com/journal/era

ERA, 33(10): 6096–6140.
DOI: 10.3934/era.2025271
Received: 20 July 2025
Revised: 27 August 2025
Accepted: 22 September 2025
Published: 20 October 2025

Research article

Dynamics analysis of autonomous and nonautonomous predator-prey models with nonlinear harvesting

Xinyu Xie[1,2], Hengguo Yu[1,2,*], Jingzhe Fang[1], Zhongyang Cao[1], Qi Wang[2,3] and Min Zhao[2,3,*]

[1] School of Mathematics and Physics, Wenzhou University, Wenzhou 325035, China

[2] Key Laboratory for Subtropical Oceans & Lakes Environment and Biological Resources Utilization Technology of Zhejiang, Wenzhou University, Wenzhou 325035, China

[3] School of Life and Environmental Science, Wenzhou University, Wenzhou 325035, China

* **Correspondence:** Email: yuhengguo5340@163.com, zhaomin-zmcn@tom.com.

Abstract: In the paper, autonomous and nonautonomous predator-prey models with nonlinear harvesting and Beddington-DeAngelis functional response were proposed. The mathematical goal was to explore the evolution process of specific bifurcation dynamics, the existence, and attractiveness of positive periodic solutions. The ecological objective was to ascertain the population growth coexistence modes and their underlying driving mechanisms from a specific perspective of dynamic evolution. Regarding the autonomous predator-prey model, mathematical theoretical work has investigated the existence and local stability of all equilibrium points, as well as the occurrence of specific bifurcation dynamics. Regarding the nonautonomous predator-prey model, the boundedness of all solutions, the possibility and global attractiveness of a positive periodic solution were theoretically derived in detail. The numerical simulation work not only verified the feasibility of the theoretical derivation work, but also dynamically showed that the autonomous model had transcritical bifurcation, saddle-node bifurcation, Hopf bifurcation, and Bogdanov-Takens bifurcation, while the nonautonomous model had attractive periodic solutions. It was worth emphasizing that predator and prey had steady state constant growth coexistence mode and steady state periodic oscillation growth coexistence mode. It must also be pointed out that their intrinsic driving mechanisms were mainly the specific bifurcation dynamics evolution mechanism in autonomous model and seasonal disturbance of key ecological environment parameters in the nonautonomous model. In summary, it was expected that these research results would contribute to the rapid development of nonlinear dynamics in predator-prey models.

Keywords: predator-prey model; nonlinear harvesting; periodic solution; Bifurcation; coexistence mode

1. Introduction

The first predator-prey model was proposed by mathematicians Lotka [1] and Volterra [2], which can explain the interaction mechanism between prey and predator. This predator-prey model has been widely used by numerous biologists and mathematicians to investigate the complex dynamic behaviors of ecological models. Moreover, as population growth functions and interaction functional responses are two critical factors in predator-prey models, the Leslie-Gower model [3, 4] introduced improvements to the Lotka-Volterra predator-prey model, with its general form being:

$$\begin{cases} \frac{dx}{dt} = rx(1 - \frac{x}{K}) - y\Phi(x, y), \\ \frac{dy}{dt} = sy(1 - \frac{y}{hx}), \end{cases} \tag{1.1}$$

where x and y represent the densities of prey and predator, respectively; $\Phi(x, y)$ denotes the interaction functional response; r and s are the per capita intrinsic growth rate of prey and predator; K is the carrying capacity for the prey; and h evaluates the conversion of prey food quality into predator birth rates.

In natural environments, most predators feed on multiple prey species rather than a single one, enabling them to persist in ecosystems even if a specific prey species is missing. Thus, predator growth can also be represented by the Beverton–Holt function. Erbach [5] studied the system dynamics of generalist predators with S-shaped functional responses, dynamic prey populations, and fixed alternative food sources, revealing that the system can exhibit up to six steady states, bistability, limit cycle oscillations, and multiple global bifurcation behaviors. Mandal [6] and Mondal [7] respectively investigated the dynamical behavioral changes of the system under the dual influences of prey refuge behavior and predator alternative food sources, as well as hunting cooperation and predator alternative food sources.

As is well known, many ecological environmental factors can affect the nonlinear dynamic evolution process of predator-prey ecological models, such as activation function, Allee effect, delay, risk effect, harvesting, fear, habitat selection, and diffusion et al. Cai [8] studied a Leslie-Gower predator-prey model with additive Allee effect in prey, finding that it can increase ecological extinction risk. Sen [9] showed that a generalized predator-prey model with Allee effect could exhibit stronger structural stability and simpler dynamics as the Allee parameter value increased, compared to models without Allee effects. Jia [10] considered a predator-prey with weak Allee effect to explore the canard cycle and relaxation oscillation. Shang [11] established a predator-prey model with double Allee effect and nonlinear harvesting to investigate multiple bifurcation, such as transcritical bifurcation, saddle-node bifurcation, and Bogdanov-Takens bifurcation. Wang [12, 13] constructed a predator-prey model incorporating fear costs in prey reproduction, verifying that higher prey birth rates or predator death rates can reduce prey sensitivity to predation risk, while increasing predator attack rates can enhance anti-predatory behaviors. Chen [14] found that escalating fear intensity can trigger dynamic transitions, leading to prey extinction (predators persist via alternative prey), with initial densities determining coexisting steady states or periodic oscillations. The papers [15, 16] have explored risk effects on predator-prey dynamics. The papers [17, 18] have studied the influence of the Beddington-DeAngelis functional response on predator-prey models and analyzed the changes in dynamical behaviors of the predator-prey system. The papers [19–21] mainly investigated stability and bifurcation of the predator-prey model with Michaelis-Menten type harvesting. Hu [22] found

delay-dependent Hopf curves, which can induce the coexistence of two limit cycles with different frequencies. Zhang [23] proposed a predator-prey model with density-dependent diffusion to study the existence, stability, and local bifurcation of the semi-trivial steady-state solution. Ding [24] formulated a phytoplankton-zooplankton model with time delay in the herd-taxis effect diffusion to research Turing-Hopf bifurcation. Mondal [25] revealed that increasing predator harvesting rates could induce up to four interior equilibrium points via saddle-node bifurcation, including catastrophic transitions that could destabilize the system. Tian [26, 27] introduced habitat selection and refuge effect respectively to propose the new prey-predator model, where they found that habitat selection can affect species locations and suitable living environments, and different dynamic behaviors can be obtained in the system with discontinuous refuge. Yan [28] constructed a fishery prey-predator model with fear effect to investigate hybrid effect of cooperative hunting and inner fear. Ch-Chaoui [29, 30] built a prey-predator model with prey Allee effect and predator-induced fear, and they provided novel insights into the interplay between fear dynamics, Allee effect, and ecological stability. Mokni [31] proposed a new single and multi-species evolutionary competition model to require a more advanced mathematical theory to handle effectively. Zhu [32–36] proposed several types of neural network models to explore Turing instability, Turing bifurcation, and Turing patterns. He [37] studied the influence of saturated fear effects on species dynamics based on the Lotka-Volterra competition model. In summary, the aforementioned scholars have made numerous outstanding achievements in ecological mathematical models.

Seasonal factors could play a crucial role in predator-prey models, which shaped ecological dynamics by altering resource availability, habitat quality, and predation pressure [38]. Many studies [39–41] have explored the seasonal impacts of fear by constructing nonautonomous ecological models, deriving sufficient conditions for the existence of at least one positive periodic solution in seasonally driven systems. Based on the assumption that predator populations follow the Beverton–Holt equation, Tang [42] investigated impulsive harvesting strategies in seasonal environments, focusing on the dual dimensions of economic effects and resource sustainability. Feng [43] and Liu [44] studied seasonal predator-prey models with Michaelis-Menten type harvesting, and analyzed the impact of seasonal disturbances on the dynamic behavior. Roy [33] analyzed the effects of seasonal disturbances in the birth rate of bait and the degree of hunting cooperation on dynamic behavior.

In this paper, we considered the following assumptions.

A1. In the absence of predator population, the prey population can grow at a constant growth rate r. Due to the limited resources required for survival and reproduction, there is competition among the prey species. m_1 is the mortality rate of the prey x due to other causes. Besides, $\frac{r}{K}x^2$ can be regarded as the part that leads to the reduction of the population size due to environmental carrying capacity, where K indicates the environmental capacity of prey population.

A2. Predators are generalists. If their favorite prey is unavailable, they can switch among different prey species. To simulate the growth of predators obtaining sustenance from other food resources when their preferred food resources are lacking, we adopted the Beverton-Holt functional form $\frac{\alpha y}{1+\beta y}$, where α and β represent the per-capita reproduction rate and the density-dependent intensity of predators, respectively. The natural mortality rate of carnivores is m_2.

A3. Prey species can expend more energy on behaviors to defend against predators, which leads to an increase in the cost of fear and a reduction in the reproduction rate. Therefore, we take the fear

factor into account as $\frac{1}{1+my}$, where m represents the level of fear.

A4. The speed at which predators capture prey is simulated by the Beddington-DeAngelis functional response model $\frac{\lambda x}{a+x+by}$, which includes individuals of the predator species competing for the same prey. Here, λ, a, and b represent the maximum predation rate, the saturation constant, and the mutual interference among predators, respectively. Additionally, $\frac{\delta\lambda xy}{a+x+by}$ represents the influence of the Beddington-DeAngelis functional response on the increase in the number of predators through the process of feeding on prey, where δ represents the coefficient that converts the amount of prey captured into the birth rate of predators.

A5. We consider the Michaelis-Menten type harvesting of the prey population, which is given by $\frac{q_1e_1x}{c_1e_1+c_2x}$. Here, q_1 is the coefficient of harvesting ability, e_1 is the harvest amount of the prey population, and c_1, c_2 is a positive constant.

Table 1. Biological meaning of parameters describing model (1.2).

Parameters	Descriptions	Ranges
r	Intrinsic growth rate of prey populatuon	$(0, 1)$
K	The environmental capacity of prey population	$[0, 10]$
m	The level of fear	$[0, 1)$
λ	The maximum predation rate	$[0, 1)$
a	The saturation constant	$[0, 5)$
b	The mutual interference among predators	$[0, 1)$
q_1	The coefficient of harvesting ability	$[0, 1)$
e_1	The harvest amount of prey population	$[0, 1)$
c_1	Positive constant	$[0, 2)$
c_2	Positive constant	$[0, 2)$
m_1	Prey mortality from other causes	$[0, 1)$
δ	Conversion efficiency of prey biomass into predator biomass	$[0, 1)$
α	The per-capita reproduction rate	$[0, 1)$
β	The density-dependent intensity of predators	$[0, 1)$
m_2	Natural mortality rate of predator population	$[0, 1)$

Based on the above assumptions, we can construct a new predator-prey model, and it can be represented as follows:

$$\begin{cases} \frac{\mathrm{d}x}{\mathrm{d}t} = \frac{rx(1-\frac{x}{K})}{1+my} - \frac{\lambda xy}{a+x+by} - \frac{q_1e_1x}{c_1e_1+c_2x} - m_1x := F_1(x, y), \\ \frac{\mathrm{d}y}{\mathrm{d}t} = \frac{\delta\lambda xy}{a+x+by} + \frac{\alpha y}{1+\beta y} - m_2y := F_2(x, y). \end{cases} \tag{1.2}$$

This paper is divided into several parts. In the next section, we will explore an autonomous predator-prey model. Specifically, in Section 2.1, we prove that the solutions are bounded. In Sections 2.2 and 2.3, the existence and stability of the equilibrium points are discussed. In Section 2.4, various bifurcation forms of the model (1.2) are studied, including transcritical bifurcation, saddle-node bifurcation, Hopf bifurcation and codimension-2 Bogdanov-Takens bifurcation. In Section 3, we will study the nonautonomous predator-prey model and consider time-varying parameters. Among them, in Section 3.1, it is proved that the solutions are bounded. In Sections 3.2 and 3.3, the existence of positive periodic solutions is proved and they are shown to be

globally attractive. In Section 4, in order to better verify the correctness of theoretical derivations and demonstrate these dynamic characteristics, numerical simulation experiments of the model (1.2) and model (3.1) are presented. Finally, a brief conclusion is given in the last section.

2. The autonomous model

2.1. Posity and boundedness of the solutions

Lemma 2.1. (The standard comparison lemma) [39] Considering the scalar differential equation

$$\dot{u} = f(t,u), \quad u(t_0) = u_0,$$

where $f(t,u)$ is continuous in t and locally Lipschitz in u, for all $t > 0$ and all $u \in J \subset R$. Let $[t_0, T)$ (T could be infinity) be the maximal interval of existence of the solution $u(t)$, and suppose $u(t) \in J$ for all $t \in [t_0, T)$. Let $v(t)$ be a continuous function whose upper righthand derivative $D^+v(t)$ satisfies the differential inequality

$$D^+v(t) \le f(t, v(t)), \quad v(t_0) \le u_0,$$

with $v(t) \in J$ for all $t \in [t_0, T)$. Then, $v(t) \le u(t)$ for all $t \in [t_0, T)$.

Theorem 2.1. The solutions of the model (1.2) are always positive with the initial conditions $(x(0), y(0)) \in \Omega = \left\{(x,y) \in R^2 | x > 0, y > 0\right\}$.

Proof. Clearly, the solutions of the model (1.2) can be written in the following form:

$$\begin{aligned} x(t) &= x(0) exp\left\{\int_0^t \left[\frac{r(1-\frac{x(\xi)}{K})}{1+my(\xi)} - \frac{\lambda y(\xi)}{a+x(\xi)+by(\xi)} - \frac{q_1 e_1}{c_1 e_1 + c_2 x(\xi)} - m_1\right] \mathrm{d}\xi\right\}, \\ y(t) &= y(0) exp\left\{\int_0^t \left[\frac{\delta\lambda x(\xi)}{a+x(\xi)+by(\xi)} - \frac{\alpha}{1+\beta(\xi)} - m_2\right] \mathrm{d}\xi\right\}. \end{aligned} \tag{2.1}$$

So according to the initial condition$(x(0), y(0)) \in \Omega = \left\{(x,y) \in R^2 | x > 0, y > 0\right\}$, all solutions of the model (1.2) must be positive. □

Theorem 2.2. The model (1.2) is uniformly ultimately bounded in R^2_+.

Proof. From the equation of the model (1.2), we can get the following inequalities

$$\frac{\mathrm{d}x}{\mathrm{d}t} \le rx(1 - \frac{x}{K}) - m_1 x = x(r - m_1 - \frac{r}{K}x), \tag{2.2}$$

and according to Lemma 2.1, we discuss the case of $r - m_1$.

If $r - m_1 \le 0$, then $\dot{x} \le 0$, so it is clear that $\lim\limits_{t\to\infty} x(t) = 0$. Then, when t is sufficiently large, we can have

$$\frac{\mathrm{d}y}{\mathrm{d}t} = \frac{\alpha y}{1+\beta y} - m_2 y = \frac{y}{1+\beta y}(\alpha - m_2 - m_2\beta y),$$

therefore, the following two situations may occur.

(i) If $\alpha - m_2 \le 0$, then $\dot{y} \le 0$, and we have $\lim\limits_{t\to\infty} y(t) = 0$, which implies that $(0,0)$ is globally asymptotically stable.

(ii) If $\alpha - m_2 > 0$, then we have $\lim\limits_{t\to\infty} y(t) = \frac{\alpha - m_2}{m_2\beta}$, which implies that $(0, \frac{\alpha - m_2}{m_2\beta})$ is globally asymptotically stable.

If $r - m_1 > 0$, by applying the Lemma 2.1, the inequality (2.2) signifies that $\lim\limits_{t\to\infty} supx(t) \le \hat{x}$, where $\hat{x}$ are positive real roots of equation

$$r - m_1 - \frac{r}{K}x = 0. \tag{2.3}$$

Also, according to $\lim\limits_{t\to\infty} supx(t) \le \hat{x}$ and the equation of the model (1.2), we can get

$$\frac{\mathrm{d}y}{\mathrm{d}t} \le \frac{\delta\lambda\hat{x}}{b} + \frac{\alpha}{\beta} - m_2 y. \tag{2.4}$$

In the same way, by using Lemma 2.1, the inequality (2.4) signifies that $\lim\limits_{t\to\infty} supy(t) \le \hat{y}$, where $\hat{y}$ are positive real roots of equation

$$\frac{\delta\lambda\hat{x}}{b} + \frac{\alpha}{\beta} - m_2 y = 0. \tag{2.5}$$

Solving the Eqs (2.3) and (2.5), we obtain $\hat{x} = \frac{(r-m_1)K}{r}$ and $\hat{y} = \frac{1}{m_2}(\frac{\delta\lambda\hat{x}}{b} + \frac{\alpha}{\beta})$. Hence, $\hat{x}$ and $\hat{y}$ are positive if $r - m_1 > 0$.

Moreover, these findings regarding the boundary equilibrium point ought to be taken into account in Subsection 2.2. In any case, when $r - m_1 \le 0$, the solution of the model (1.2) is likewise uniformly ultimately bounded. □

Theorem 2.3. If $r - m_1 > 0$, the model (1.2) is permanent.

Proof. According to Theorem 2.2, we know that when $r - m_1 \le 0$, prey populations tend to become extinct or disappear over a long period of time. So we discuss the persistence of the model (1.2) in the case of $r - m_1 > 0$.

From the equation of the model (1.2) and $\lim\limits_{t\to\infty} supx(t) \le \hat{x}$, $\lim\limits_{t\to\infty} supy(t) \le \hat{y}$, and we can get the following inequalities

$$\frac{\mathrm{d}x}{\mathrm{d}t} \ge rx(1 - \frac{\hat{x}}{K})\frac{1}{1+m\hat{y}} - \lambda\hat{y} - \frac{q_1 e_1}{c_2} - m_1\hat{x}. \tag{2.6}$$

By applying the Lemma 2.1, the inequality (2.6) signifies that $\lim\limits_{t\to\infty} infx(t) \ge \check{x}$, where $\check{x}$ are positive real roots of equation

$$rx(1 - \frac{\hat{x}}{K})\frac{1}{1+m\hat{y}} - \lambda\hat{y} - \frac{q_1 e_1}{c_2} - m_1\hat{x} = 0. \tag{2.7}$$

Also, according to $\lim\limits_{t\to\infty} infx(t) \ge \check{x}$ and the equation of the model (1.2), we can get

$$\frac{\mathrm{d}y}{\mathrm{d}t} \ge \frac{\delta\lambda\check{x}y}{a+\hat{x}+b\hat{y}} - m_2\hat{y}. \tag{2.8}$$

In the same way, by using Lemma 2.1, the inequality (2.8) signifies that $\lim\limits_{t\to\infty} infy(t) \ge \check{y}$, where $\check{y}$ are positive real roots of equation

$$\frac{\delta\lambda\check{x}y}{a+\hat{x}+b\hat{y}} - m_2\hat{y} = 0. \tag{2.9}$$

Solve the Eqs (2.7) and (2.9), we obtain $\check{x} = \frac{(\lambda\hat{y}+\frac{q_1e_1}{c_2}+m_1\hat{x})(1+m\hat{y})}{r(1-\frac{\hat{x}}{K})}$ and $\check{y} = \frac{m_2\hat{y}(a+\hat{x}+b\hat{y})}{\delta\lambda\check{x}}$. Hence $\check{x}$ and $\check{y}$ are positive, which guarantees that the model (1.2) is permanent when $r - m_1 > 0$. □

2.2. Existence of equilibria

In this paper, we analyze the zero growth isoclines $F_1(x, y) = 0$ and $F_2(x, y) = 0$ to discuss the existence of the ecological meaning equilibrium point of the model (1.2). The model (1.2) has the following four balance points.

(1) Population-free equilibrium point $E_0 = (0, 0)$, which always exists.

(2) Prey-free equilibrium point $E_1 = (0, y_1)$, where y_1 is the positive root of the following equation:

$$-m_2 y + \frac{\alpha y}{1+\beta y} = 0,$$

if $\alpha - m_2 > 0$, the equation has a positive root, which can be given by $y_1 = \frac{1}{\beta}(\frac{\alpha}{m_2} - 1)$.

(3) Predator-free equilibrium point $E_{2i} = (x_{2i}, 0)$ $(i = 1, 2, 3, 4)$, where x_{2i} is the positive root of the following equation:

$$a_2 x^2 + a_1 x + a_0 = 0,$$

where $a_2 = -\frac{rc_2}{K}, a_1 = rc_2 - \frac{rc_1 e_1}{K} - m_1 c_2, a_0 = e_1(rc_1 - q_1 - m_1 c_1)$.

The above equation has either no or one or two positive root(s), which can be discussed in the following:

(i) If $a_1 \le 0$ and $a_0 \le 0$ i.e., $\frac{(r-m_1)c_2 K}{e_1} \le rc_1 \le q_1 + m_1 c_1$ or $a_1^2 - 4a_2 a_0 < 0$, then the above equation has no positive roots. Thus, the model (1.2) does not have any predator-free equilibrium point.

(ii) If $a_1 > 0$ and $a_0 \ge 0$ (i.e., $q_1 + m_1 c_1 \le rc_1 \le \frac{(r-m_1)c_2 K}{e_1}$) or $a_1 > 0$ and $a_1^2 - 4a_2 a_0 = 0$, then the above equation has one positive root x_{21}, which is given by $x_{21} = \frac{-a_1 + \sqrt{a_1^2 - 4a_2 a_0}}{2a_2}$. Thus, the model (1.2) has a unique predator-free equilibrium point E_{21}.

(iii) If $a_1 = 0$ and $a_0 > 0$ (i.e., $r = m_1$ and $rc_1 > q_1 + m_1 c_1$) or $a_1 < 0$ and $a_0 > 0$ (i.e., $rc_1 > max\left\{q_1 + m_1 c_1, \frac{(r-m_1)c_2 K}{e_1}\right\}$), then the above equation has one positive root x_{22}, which is given by $x_{22} = \frac{-a_1 + \sqrt{a_1^2 - 4a_2 a_0}}{2a_2}$. Thus, the model (1.2) has a unique predator-free equilibrium point E_{22}.

(iv) If $a_1 > 0$, $a_0 < 0$ and $a_1^2 - 4a_2 a_0 > 0$ (i.e. $rc_1 < min\left\{q_1 + m_1 c_1, \frac{(r-m_1)c_2 K}{e_1}\right\}$ and $a_1^2 - 4a_2 a_0 > 0$), then the above equation has two positive roots x_{23} and x_{24}, which is given by $x_{23} = \frac{-a_1 - \sqrt{a_1^2 - 4a_2 a_0}}{2a_2}$ and $x_{24} = \frac{-a_1 + \sqrt{a_1^2 - 4a_2 a_0}}{2a_2}$. Thus, the model (1.2) has two predator-free equilibrium points E_{23} and E_{24}.

(4) The internal equilibrium point is $E^* = (x^*, y^*)$, which is the intersection of nontrivial zero growth isoclines $F_1(x, y) = 0$ and $F_2(x, y) = 0$. From $F_2(x, y) = 0$, we can get $x^* = \frac{m_2(a+by^*)(1+\beta y^*) - \alpha(a+by^*)}{\delta\lambda(1+\beta y^*) - m_2(1+\beta y^*) + \alpha}$.

Earlier we used y^* for x^*. To simplify calculations, we let

$$Q_1(y) = \delta\lambda(1 + \beta y) - m_2(1 + \beta y) + \alpha = c_{11} y + c_{12},$$

$$Q_2(y) = m_2(a + by)(1 + \beta y) - \alpha(a + by) = d_{11} y^2 + d_{12} y + d_{13},$$

where $c_{11} = (\delta\lambda - m_2)\beta$, $c_{12} = \delta\lambda - m_2 + \alpha$, $d_{11} = b\beta m_2$, $d_{12} = b(m_2 - \alpha) + a\beta m_2$, $d_{13} = a(m_2 - \alpha)$, then the equation can be simplified as $x^* = \frac{Q_2(y^*)}{Q_1(y^*)}$.

From $F_1(x, y) = 0$, we can get

$$A_1 x^3 + A_2 x^2 + A_3 x^2 y + A_4 x + A_5 xy + A_6 xy^2 + A_7 y + A_8 y^2 + A_9 = 0,$$

where

$$A_1 = -rc_2, \quad A_2 = r(Kc_2 - ac_2 - c_1 e_1) - m_1 Kc_2, \quad A_3 = c_2(-br - mm_1 K),$$
$$A_4 = r(Kac_2 + Kc_1 e_1 - ac_1 e_1) - Kq_1 e_1 - m_1 K(ac_2 + c_1 e_1),$$
$$A_5 = r(Kbc_2 - bc_1 e_1) - K\lambda c_2 - Kq_1 e_1 m - m_1 K\left[bc_2 + m(ac_2 + c_1 e_1)\right], \quad A_6 = Km(-\lambda c_2 - m_1 c_2 b),$$
$$A_7 = Kc_1 e_1\left[rb - \lambda - m_1(am + b)\right] - Kq_1 e_1(am + b), \quad A_8 = -Km(\lambda c_1 e_1 + m_1 bc_1 e_1 + bq_1 e_1),$$
$$A_9 = Kac_1 e_1(r - m_1) - Kaq_1 e_1,$$

therefore, y^* is the positive root of the following equation:

$$f(y) = B_6y^6 + B_5y^5 + B_4y^4 + B_3y^3 + B_2y^2 + B_1y + B_0 = 0,$$

where

$$\begin{aligned}
B_6 &= A_1d_{11}^3 + A_3c_{11}d_{11}^2 + A_6c_{11}^2d_{11},\\
B_5 &= 3A_1d_{11}^2d_{12} + A_2c_{11}d_{11}^2 + 2A_3c_{11}d_{11}d_{12} + A_3c_{12}d_{11}^2 + A_5c_{11}^2d_{11} + A_6c_{11}^2d_{12} + 2A_6c_{11}c_{12}d_{11} + c_{11}^3A_8,\\
B_4 &= 3A_1d_{11}^2d_{13} + 3A_1d_{11}d_{12}^2 + 2A_2c_{11}d_{11}d_{12} + A_2c_{12}d_{11}^2 + 2A_3c_{11}d_{11}d_{13} + A_3c_{11}d_{12}^2 + 2A_3c_{12}d_{11}d_{12}\\
&\quad + A_4c_{11}^2d_{11} + A_5c_{11}^2d_{12} + 2A_5c_{11}c_{12}d_{11} + A_6c_{11}^2d_{13} + 2A_6c_{11}c_{12}d_{12} + A_6c_{12}^2d_{11} + c_{11}^3A_7 + 3A_8c_{11}^2c_{12},\\
B_3 &= 6d_{11}d_{12}d_{13}A_1 + d_{12}^3A_1 + 2A_2c_{11}d_{11}d_{13} + A_2c_{11}d_{12}^2 + 2A_2c_{12}d_{11}d_{12} + 2A_3c_{11}d_{12}d_{13} + 2A_3c_{12}d_{11}d_{13}\\
&\quad + A_3c_{12}d_{12}^2 + A_4c_{11}^2d_{12} + 2A_4c_{11}c_{12}d_{11} + A_5c_{11}^2d_{13} + 2A_5c_{11}c_{12}d_{12} + A_5c_{12}^2d_{11} + 2A_6c_{11}c_{12}d_{13}\\
&\quad + A_6c_{12}^2d_{12} + 3A_7c_{11}^2c_{12} + 3A_8c_{11}c_{12}^2 + A_9c_{11}^3,\\
B_2 &= 3A_1d_{11}d_{13}^2 + 3A_1d_{12}^2d_{13} + 2A_2c_{11}d_{12}d_{13} + 2A_2c_{12}d_{11}d_{13} + A_2c_{12}d_{12}^2 + A_3c_{11}d_{13}^2 + 2A_3c_{12}d_{12}d_{13}\\
&\quad + A_4c_{11}^2d_{13} + 2A_4c_{11}c_{12}d_{12} + A_4c_{12}^2d_{11} + 2A_5c_{11}c_{12}d_{13} + A_5c_{12}^2d_{12} + A_6c_{12}^2d_{13} + 3A_7c_{11}c_{12}^2 + c_{12}^3A_8\\
&\quad + 3A_9c_{11}^2c_{12},\\
B_1 &= 3d_{12}d_{13}^2A_1 + A_2c_{11}d_{13}^2 + 2A_2c_{12}d_{12}d_{13} + A_3c_{12}d_{13}^2 + 2A_4c_{11}c_{12}d_{13} + A_4c_{12}^2d_{12} + A_5c_{12}^2d_{13}\\
&\quad + c_{12}^3A_7 + 3A_9c_{11}c_{12}^2,\\
B_0 &= A_1d_{13}^3 + A_2c_{12}d_{13}^2 + A_4c_{12}^2d_{13} + A_9c_{12}^3.
\end{aligned}$$

The root of deterministic equation is quite complex. Therefore, we find all the internal equilibrium points of the model (1.2) numerically. To do this, we draw the nontrivial prey and predator isoclines ($F_1(x, y) = 0$ and $F_1(x, y) = 0$) and the image of $f(y)$. From Figure 1(a) and 2(a), it is apparent that for $\alpha = 0.25$, there is no internal equilibrium point. When $\alpha = 0.2227608967$, the model (1.2) has a positive internal equilibrium point E_+. From Figure1(b), and in Figure 2(b), y_+ is a dual positive root. In Figure 1(c), we can observe that the model (1.2) has two internal equilibrium points $E_1^* = (x_1^*, y_1^*)$, $E_2^* = (x_2^*, y_2^*)$, with $y_1^* < y_2^*$, when $\alpha = 0.21$, moreover, y_1^* and y_2^* are all single positive roots in Figure 2(c). Further, while $\alpha = 0.18$, the model (1.2) has a unique internal equilibrium point E_3^* in Figure 1(d), where y_3^* is a single positive root in Figure 2(d).

Table 2. Parameter values.

r	K	m	λ	a	b	q_1	e_1	c_1	c_2	m_1	δ	β	m_2
0.8	10	0.2	0.5	2	0.2	0.2	0.25	0.3	0.1	0.2	0.15	0.3	0.2

2.3. Stability of equilibria

In this section, we explore the stability of the equilibria.The Jacobian matrix of the model (1.2) is:

$$J(x, y) = \begin{pmatrix} J_{11} & J_{12} \\ J_{21} & J_{22} \end{pmatrix},$$

where

$$\begin{aligned}
J_{11} &= \tfrac{r(1-\frac{2x}{K})}{1+my} - \tfrac{\lambda y(a+by)}{(a+x+by)^2} - \tfrac{q_1e_1^2c_1}{(c_1e_1+c_2x)^2} - m_1, \quad J_{12} = -rx(1-\tfrac{x}{K})\tfrac{m}{(1+my)^2} - \tfrac{\lambda x(a+x)}{(a+x+by)^2},\\
J_{21} &= \tfrac{\delta\lambda y(a+by)}{(a+x+by)^2}, \quad J_{22} = \tfrac{\delta\lambda x(a+x)}{(a+x+by)^2} - m_2 + \tfrac{\alpha}{(1+\beta y)^2}.
\end{aligned}$$

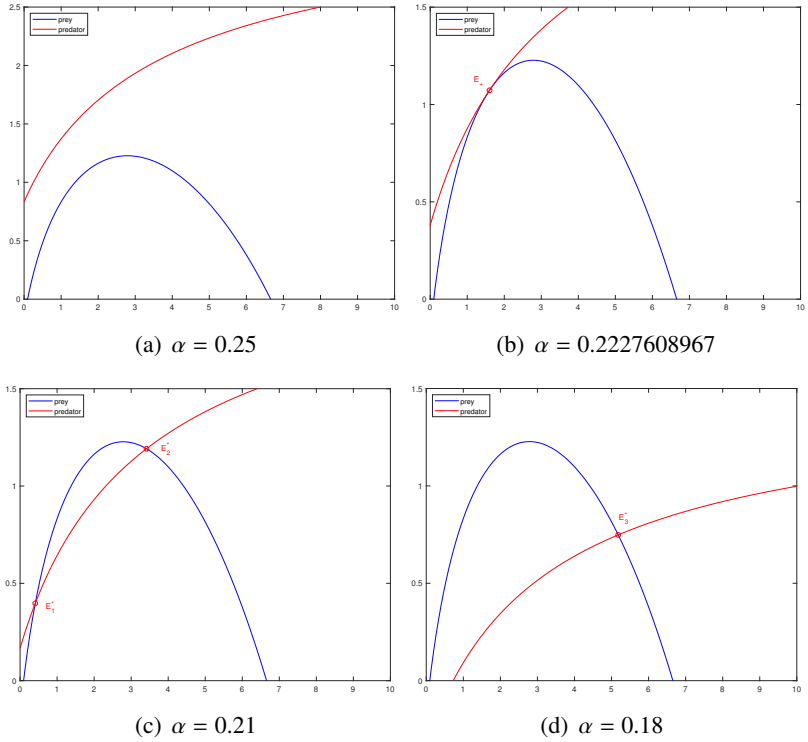

(a) $\alpha = 0.25$ (b) $\alpha = 0.2227608967$

(c) $\alpha = 0.21$ (d) $\alpha = 0.18$

Figure 1. A description of the intersection of the prey and predator zero growth isoslashes with different values of α. The reaming parameters remain the same as the values specified in Table 2. (a) $\alpha = 0.25$, there is no intersection; (b) $\alpha = 0.2227608967$, there is an intersection; (c) $\alpha = 0.21$, there are two intersections; (d) $\alpha = 0.18$, there is an intersection.

2.3.1. Stability at the origin

Theorem 2.4. The stability at the origin $E_0(0, 0)$ is discussed as follows:

(1) If $(r - \frac{q_1}{c_1} - m_1)(\alpha - m_2) < 0$, then E_0 is a saddle.

(2) If $(r - \frac{q_1}{c_1} - m_1)(\alpha - m_2) > 0$, then E_0 is a node. When $r - \frac{q_1}{c_1} - m_1 < 0$ and $\alpha < m_2$, E_0 is a stable node; when $r - \frac{q_1}{c_1} - m_1 > 0$ and $\alpha > m_2$, E_0 is an unstable node.

(3) If $\alpha - m_2 = 0$, then E_0 is a saddle-node.

Proof. The Jacobian matrix of E_0 is:

$$J_{E_0} = \begin{pmatrix} r - \frac{q_1}{c_1} - m_1 & 0 \\ 0 & \alpha - m_2 \end{pmatrix}.$$

Apparently J_{E_0} has two eigenvalues, $\mu_1 = r - \frac{q_1}{c_1} - m_1$ and $\mu_2 = \alpha - m_2$. Hence, if $\mu_1 > 0$ and $\mu_2 < 0$ or $\mu_1 < 0$ and $\mu_2 > 0$, i.e., $(r - \frac{q_1}{c_1} - m_1)(\alpha - m_2) < 0$, then E_0 is a saddle; if $\mu_1 > 0$ and $\mu_2 > 0$, i.e., $r - \frac{q_1}{c_1} - m_1 > 0$ and $\alpha - m_2 > 0$, then E_0 is an unstable node; if $\mu_1 < 0$ and $\mu_2 < 0$, i.e., $r - \frac{q_1}{c_1} - m_1 < 0$ and $\alpha - m_2 < 0$, then E_0 is a stable node.

If $\alpha - m_2 = 0$, then J_{E_0} will only have a zero eigenvalue, $\mu_1 = r - \frac{q_1}{c_1} - m_1 \neq 0$ and $\mu_2 = 0$. Meanwhile,

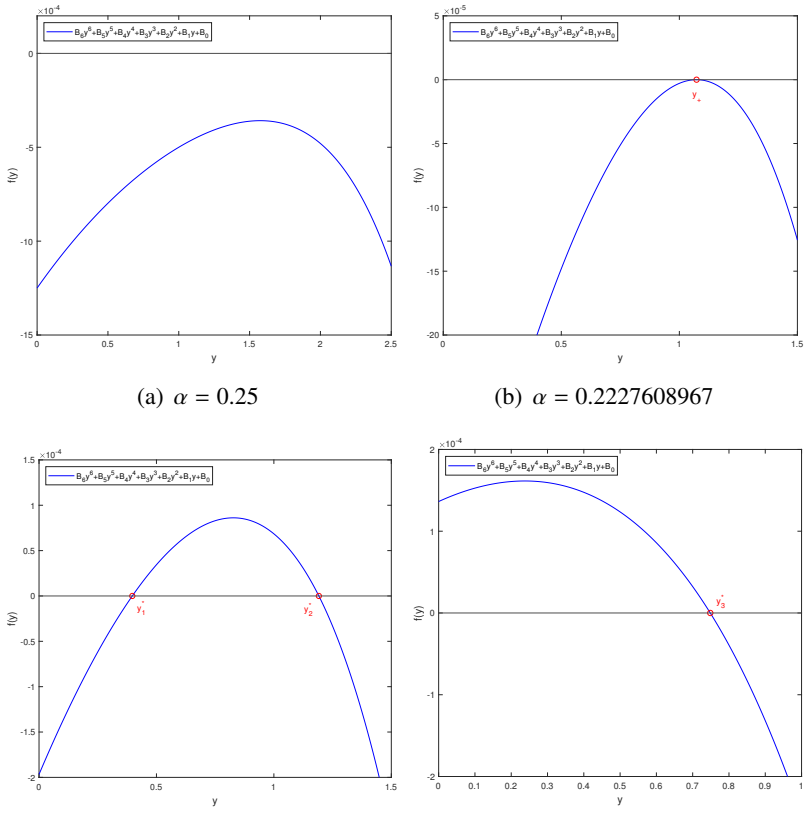

(a) $\alpha = 0.25$ (b) $\alpha = 0.2227608967$

(c) $\alpha = 0.21$ (d) $\alpha = 0.18$

Figure 2. A description of the value of $f(y)$ with different values of α. The reaming parameters remain the same as the values specified in Table 2. (a) $\alpha = 0.25$, there is no positive root; (b) $\alpha = 0.2227608967$, there is a dual positive root; (c) $\alpha = 0.21$, there are two single positive roots; (d) $\alpha = 0.18$, there is a single positive root.

we expand the model (1.2) near the origin to the third order, then the model (1.2) becomes

$$\begin{cases} \dot{X} = (r - \frac{q_1}{c_1} - m_1)X + (rm - \frac{\lambda}{a})XY + (-\frac{r}{K} + \frac{q_1 c_2}{c_1^2 e_1})X^2 - \frac{q_1 e_2^2}{c_1^3 e_1^2}X^3 + (\frac{rm}{K} + \frac{\lambda}{a^2})X^2 Y \\ \qquad +(rm^2 + \frac{\lambda b}{a^2})XY^2 + P_1(X, Y), \\ \dot{Y} = \frac{\delta\lambda}{a}XY - \alpha\beta Y^2 + \alpha\beta^2 X^2 Y + \frac{\delta\lambda}{a^2}XY^2 + \frac{\delta\lambda b}{a^2}Y^3 + Q_1(X, Y), \end{cases} \tag{2.10}$$

where $P_1(X, Y)$ and $Q_1(X, Y)$ are C^∞ functions at least of order fourth in (X, Y).

Introducing a new variable τ through $\tau = (r - \frac{q_1}{c_1} - m_2)$, we have

$$\begin{cases} \dot{X} = X + \frac{rm - \frac{\lambda}{a}}{r - \frac{q_1}{c_1} - m_2}XY + (-\frac{r}{K(r - \frac{q_1}{c_1} - m_2)} + \frac{q_1 c_2}{c_1^2 e_1 (r - \frac{q_1}{c_1} - m_2)})X^2 - \frac{q_1 e_2^2}{c_1^3 e_1^2 (r - \frac{q_1}{c_1} - m_2)}X^3 + (\frac{rm}{K(r - \frac{q_1}{c_1} - m_2)} + \frac{\lambda}{a^2(r - \frac{q_1}{c_1} - m_2)})X^2 Y \\ \qquad +(\frac{rm^2}{r - \frac{q_1}{c_1} - m_2} + \frac{\lambda b}{a^2 r - \frac{q_1}{c_1} - m_2})XY^2 + P_2(X, Y), \\ \dot{Y} = \frac{\delta\lambda}{a(r - \frac{q_1}{c_1} - m_2)}XY - \frac{\alpha\beta}{r - \frac{q_1}{c_1} - m_2}Y^2 + \frac{\alpha\beta^2}{r - \frac{q_1}{c_1} - m_2}X^2 Y + \frac{\delta\lambda}{a^2(r - \frac{q_1}{c_1} - m_2)}XY^2 + \frac{\delta\lambda b}{a^2(r - \frac{q_1}{c_1} - m_2)}Y^3 + Q_2(X, Y), \end{cases} \tag{2.11}$$

where $P_2(X, Y)$ and $Q_2(X, Y)$ are C^∞ functions at least of order fourth in (X, Y). Therefore, the

coefficient of Y^2 in the second equation of the model (2.11) is $-\frac{\alpha\beta}{r-\frac{q_1}{c_1}-m_2} \neq 0$, then E_0 is a saddle-node in Theorem 7.1 of Chapter 2 of the paper [46]. □

2.3.2. Stability of boundary equilibrium point

Theorem 2.5. The stability of boundary equilibrium point $E_1(0, y_1)$ is discussed as follows:

(1) If $(\frac{r}{1+my_1} - \frac{\lambda y_1}{a+by_1} - \frac{q_1}{c_1} - m_1)(\alpha - m_2) > 0$, then E_1 is a saddle.

(2) If $(\frac{r}{1+my_1} - \frac{\lambda y_1}{a+by_1} - \frac{q_1}{c_1} - m_1)(\alpha - m_2) < 0$, then E_1 is a node. When $\frac{r}{1+my_1} - \frac{\lambda y_1}{a+by_1} - \frac{q_1}{c_1} - m_1 > 0$ and $m_2 > \alpha$, E_1 is an unstable node; when $\frac{r}{1+my_1} - \frac{\lambda y_1}{a+by_1} - \frac{q_1}{c_1} - m_1 < 0$ and $m_2 < \alpha$, E_1 is a stable node.

(3) If $\alpha - m_2 = 0$, then E_1 is a saddle-node.

Proof. The Jacobian matrix of E_1 is:

$$J_{E_1} = \begin{pmatrix} \frac{r}{1+my_1} - \frac{\lambda y_1}{a+by_1} - \frac{q_1}{c_1} - m_1 & 0 \\ \frac{\delta\lambda y_1}{a+by_1} & -\frac{m_2}{\alpha}(\alpha - m_2) \end{pmatrix}.$$

Apparently J_{E_1} has two eigenvalues, $\mu_1 = \frac{r}{1+my_1} - \frac{\lambda y_1}{a+by_1} - \frac{q_1}{c_1} - m_1$ and $\mu_2 = -\frac{m_2}{\alpha}(\alpha - m_2)$. Hence, if $\mu_1 > 0$ and $\mu_2 < 0$ or $\mu_1 < 0$ and $\mu_2 > 0$, i.e., $(\frac{r}{1+my_1} - \frac{\lambda y_1}{a+by_1} - \frac{q_1}{c_1} - m_1)(\alpha - m_2) > 0$, then E_1 is a saddle; if $\mu_1 > 0$ and $\mu_2 > 0$, i.e., $\frac{r}{1+my_1} - \frac{\lambda y_1}{a+by_1} - \frac{q_1}{c_1} - m_1 > 0$ and $m_2 > \alpha$, then E_1 is an unstable node; if $\mu_1 < 0$ and $\mu_2 < 0$, i.e., $\frac{r}{1+my_1} - \frac{\lambda y_1}{a+by_1} - \frac{q_1}{c_1} - m_1 < 0$ and $m_2 < \alpha$, then E_1 is a stable node.

If $\alpha - m_2 = 0$, then J_{E_1} will only have a zero eigenvalue, $\mu_1 = \frac{r}{1+my_1} - \frac{\lambda y_1}{a+by_1} - \frac{q_1}{c_1} - m_1$ and $\mu_2 = 0$. We shift E_1 to the origin by $(X, Y) = (x, y - y_1)$, and expand the model (1.2) up to the third order using the Taylor series, obtaining

$$\begin{cases} \dot{X} = r_{10}X + r_{11}XY + r_{20}X^2 + r_{30}X^3 + r_{21}X^2Y + r_{12}XY^2 + P_3(X, Y), \\ \dot{Y} = h_{10}X + h_{11}XY + h_{20}X^2 + h_{02}Y^2 + h_{30}X^3 + h_{21}X^2Y + h_{12}XY^2 + h_{03}Y^3 + Q_3(X, Y), \end{cases} \tag{2.12}$$

where

$$\begin{aligned} &r_{10} = \tfrac{r}{my_1+1} - \tfrac{\lambda y_1}{by_1+a} - \tfrac{q_1}{c_1} - m_1, \quad r_{11} = -\tfrac{rm}{(my_1+1)^2} - \tfrac{\lambda a}{(by_1+a)^2}, \quad r_{20} = -\tfrac{r}{K(my_1+1)} + \tfrac{\lambda y_1}{(by_1+a)^2} + \tfrac{q_1c_2}{e_1c_1^2}, \\ &r_{30} = -\tfrac{\lambda y_1}{(by_1+a)^3} - \tfrac{q_1c_2^2}{e_1^2c_1^3}, \quad r_{21} = \tfrac{rm}{K(my_1+1)^2} + \tfrac{-\lambda(y_1b-a)}{(by_1+a)^3}, \quad r_{12} = \tfrac{rm^2}{(my_1+1)^3} + \tfrac{\lambda ab}{(by_1+a)^3}, \\ &h_{10} = \tfrac{\delta\lambda y_1}{by_1+a}, \quad h_{11} = \tfrac{\delta\lambda a}{(by_1+a)^2}, \quad h_{20} = -\tfrac{\delta\lambda y_1}{(by_1+a)^2}, \quad h_{02} = -\tfrac{\alpha\beta}{(\beta y_1+1)^3}, \quad h_{30} = \tfrac{\delta\lambda y_1}{(by_1+a)^3}, \\ &h_{03} = \tfrac{\alpha\beta^2}{(\beta y_1+1)^4}, \quad h_{21} = -\tfrac{\delta\lambda(-by_1+a)}{(by_1+a)^3}, \quad h_{12} = -\tfrac{\delta\lambda ba}{(by_1+a)^3}, \end{aligned}$$

and $P_3(X, Y)$ and $Q_3(X, Y)$ are C^∞ functions at least of order fourth in (X, Y).

By the simplistic transformation

$$\begin{pmatrix} x \\ y \end{pmatrix} = \begin{pmatrix} 1 & 0 \\ 1 & -\frac{r_{10}}{h_{10}} \end{pmatrix} \begin{pmatrix} X \\ Y \end{pmatrix},$$

the model (2.12) can be written as

$$\begin{cases} \dot{x} = a_{10}x + a_{11}xy + a_{20}x^2 + a_{30}x^3 + a_{21}x^2y + a_{12}xy^2 + P_4(x, y), \\ \dot{y} = b_{20}x^2 + b_{11}xy + b_{02}y^2 + b_{30}x^3 + b_{20}x^2y + b_{12}xy^2 + b_{03}y^3 + Q_4(x, y), \end{cases} \tag{2.13}$$

where

$$a_{10}=r_{10},\quad a_{11}=-\frac{h_{10}r_{11}}{r_{10}},\quad a_{20}=\frac{h_{10}r_{11}+r_{10}r_{20}}{r_{10}},\quad a_{30}=\frac{h_{10}^2r_{12}+h_{10}r_{10}r_{21}+r_{10}^2r_{30}}{r_{10}^2},\quad a_{21}=-\frac{h_{10}(2h_{10}r_{12}+r_{10}r_{21})}{r_{10}^2},$$
$$a_{12}=\frac{r_{12}h_{10}^2}{r_{10}^2},\quad b_{20}=-\frac{h_{02}h_{10}^2-r_{11}h_{10}^2+h_{10}h_{11}r_{10}-h_{10}r_{10}r_{20}+h_{20}r_{10}^2}{r_{10}h_{10}},\quad b_{11}=\frac{2h_{02}h_{10}-h_{10}r_{11}+h_{11}r_{10}}{r_{10}},\quad b_{02}=-\frac{h_{10}h_{02}}{r_{10}},$$
$$b_{30}=-\frac{h_{03}h_{10}^3-h_{10}^3r_{12}+h_{10}^2h_{12}r_{10}-r_{21}h_{10}^2r_{10}+h_{21}h_{10}r_{10}^2-r_{30}h_{10}r_{10}^2+h_{30}r_{10}^3}{r_{10}^2h_{10}},$$
$$b_{20}=\frac{3h_{03}h_{10}^2-2h_{10}^2r_{12}+2h_{10}h_{12}r_{10}-h_{10}r_{10}r_{21}+h_{21}r_{10}^2}{r_{10}^2},\quad b_{12}=-\frac{h_{10}(3h_{03}h_{10}-h_{10}r_{12}+h_{12}r_{10})}{r_{10}^2},\quad b_{03}=\frac{h_{03}h_{10}^2}{r_{10}^2},$$

and $P_4(x,y)$ and $Q_4(x,y)$ are C^∞ functions at least of order fourth in (x,y).

We import a new variable τ to the model (2.13) by $\tau=a_{10}t$. For formal simplicity, we still use t instead of τ. We have the standard form

$$\begin{cases}\dot{x}=x+\dfrac{a_{11}}{a_{10}}xy+\dfrac{a_{20}}{a_{10}}x^2+\dfrac{a_{30}}{a_{10}}x^3+\dfrac{a_{21}}{a_{10}}x^2y+\dfrac{a_{12}}{a_{10}}xy^2+P_5(x,y),\\ \dot{y}=\dfrac{b_{20}}{a_{10}}x^2+\dfrac{b_{11}}{a_{10}}xy+\dfrac{b_{02}}{a_{10}}y^2+\dfrac{b_{30}}{a_{10}}x^3+\dfrac{b_{20}}{a_{10}}x^2y+\dfrac{b_{12}}{a_{10}}xy^2+\dfrac{b_{03}}{a_{10}}y^3+Q_5(x,y),\end{cases}\tag{2.14}$$

where $P_4(x,y)$ and $Q_4(x,y)$ are C^∞ functions at least of order fourth in (x,y). Hence, we find that the coefficient of y^2 is $\frac{b_{02}}{a_{10}}$ for the second equation of the model (2.14), i.e., $r_{10}\neq 0$, $h_{10}\neq 0$, and $h_{02}\neq 0$, then E_1 is a saddle-node from Theorem 7.1 in Chapter 2 in the paper [46]. □

Theorem 2.6. The stability of boundary equilibrium point $E_{24}(x_{24},0)$ is discussed as follows:

(1) If $(r(1-\frac{2x_{24}}{K})-\frac{q_1e_1^2c_1}{(c_1e_1+c_2x_{24})^2}-m_1)(\frac{\delta\lambda x_{24}}{a+x_{24}}-m_2+\alpha)<0$, then E_{24} is a saddle.

(2) If $(r(1-\frac{2x_{24}}{K})-\frac{q_1e_1^2c_1}{(c_1e_1+c_2x_{24})^2}-m_1)(\frac{\delta\lambda x_{24}}{a+x_{24}}-m_2+\alpha)>0$, then E_{24} is a node. When $r(1-\frac{2x_{24}}{K})-\frac{q_1e_1^2c_1}{(c_1e_1+c_2x_{24})^2}-m_1>0$ and $\frac{\delta\lambda x_{24}}{a+x_{24}}-m_2+\alpha>0$, E_{24} is an unstable node; when $r(1-\frac{2x_{24}}{K})-\frac{q_1e_1^2c_1}{(c_1e_1+c_2x_{24})^2}-m_1<0$ and $\frac{\delta\lambda x_{24}}{a+x_{24}}-m_2+\alpha<0$, E_{24} is a stable node.

(3) If $\frac{\delta\lambda x_{24}}{a+x_{24}}+\alpha-m_2=0$ i.e., $\frac{\delta\lambda x_{24}}{a+x_{24}}=m_2-\alpha$, then E_{24} is a saddle-node.

Proof. The Jacobian matrix of E_{24} is:

$$J_{E_{24}}=\begin{pmatrix}r(1-\frac{2x_{24}}{K})-\frac{q_1e_1^2c_1}{(c_1e_1+c_2x_{24})^2}-m_1 & -mrx_{24}(1-\frac{x_{24}}{K})\\ 0 & \frac{\delta\lambda x_{24}}{a+x_{24}}-m_2+\alpha\end{pmatrix}.$$

Apparently $J_{E_{24}}$ has two eigenvalues, $\mu_1=r(1-\frac{2x_{24}}{K})-\frac{q_1e_1^2c_1}{(c_1e_1+c_2x_{24})^2}-m_1$ and $\mu_2=\frac{\delta\lambda x_{24}}{a+x_{24}}-m_2+\alpha$. Hence, if $\mu_1>0$ and $\mu_2<0$ or $\mu_1<0$ and $\mu_2>0$, i.e., $(r(1-\frac{2x_{24}}{K})-\frac{q_1e_1^2c_1}{(c_1e_1+c_2x_{24})^2}-m_1)(\frac{\delta\lambda x_{24}}{a+x_{24}}-m_2+\alpha)>0$, then E_{24} is a saddle; if $\mu_1>0$ and $\mu_2>0$, i.e., $r(1-\frac{2x_{24}}{K})-\frac{q_1e_1^2c_1}{(c_1e_1+c_2x_{24})^2}-m_1>0$ and $\frac{\delta\lambda x_{24}}{a+x_{24}}-m_2+\alpha>0$, then E_{24} is an unstable node; if $\mu_1<0$ and $\mu_2<0$, i.e., $r(1-\frac{2x_{24}}{K})-\frac{q_1e_1^2c_1}{(c_1e_1+c_2x_{24})^2}-m_1<0$ and $\frac{\delta\lambda x_{24}}{a+x_{24}}-m_2+\alpha<0$, then E_{24} is a stable node.

If $\frac{\delta\lambda x_{24}}{a+x_{24}}=m_2-\alpha$, then $J_{E_{24}}$ will only have a zero eigenvalue, $\mu_1=r(1-\frac{2x_{24}}{K})-\frac{q_1e_1^2c_1}{(c_1e_1+c_2x_{24})^2}-m_1$ and $\mu_2=0$. We shift E_{24} to the origin by $(X,Y)=(x-x_{24},y)$, and expand the model (1.2) up to the third order using the Taylor series, obtaining

$$\begin{cases}\dot{X}=i_{10}X+i_{01}Y+i_{11}XY+i_{20}X^2+i_{30}X^3+i_{21}X^2Y+i_{12}XY^2+P_6(X,Y),\\ \dot{Y}=j_{11}XY+j_{21}X^2Y+j_{12}XY^2+Q_6(X,Y),\end{cases}\tag{2.15}$$

where

$$i_{10} = r(1-\tfrac{2x_{24}}{K}) - \tfrac{q_1e_1^2c_1}{(c_1e_1+c_2x_{24})^2} - m_1, \quad i_{01} = -mrx_{24}(1-\tfrac{x_{24}}{K}), \quad i_{11} = \tfrac{-mr(K-2x_{24})}{K} - \tfrac{a\lambda}{(a+x_{24})^2},$$
$$i_{20} = -\tfrac{r}{K} + \tfrac{e_1^2q_1c_1c_2}{(c_1e_1+c_2x_{24})^3}, \quad i_{30} = -\tfrac{e_1^2q_1c_1c_2^2}{(c_1e_1+c_2x_{24})^4}, \quad i_{21} = \tfrac{rm}{K} + \tfrac{-\lambda a}{(a+x_{24})^3}, \quad i_{12} = \tfrac{rm^2(K-2x_{24})}{K} + \tfrac{b\lambda(a-x_{24})}{(a+x_{24})^3},$$
$$j_{11} = \tfrac{\delta\lambda a}{(a+x_{24})^2}, \quad j_{21} = -\tfrac{\delta\lambda a}{(a+x_{24})^3}, \quad j_{12} = -\tfrac{\delta\lambda b(a-x_{24})}{(x_{24}+a)^3},$$

and $P_6(X, Y)$ and $Q_6(X, Y)$ are C^∞ functions at least of order fourth in (X, Y).

By the simplistic transformation

$$\begin{pmatrix} x \\ y \end{pmatrix} = \begin{pmatrix} 1 & \frac{i_{01}}{i_{10}} \\ 0 & 1 \end{pmatrix} \begin{pmatrix} X \\ Y \end{pmatrix},$$

the model (2.15) can be written as

$$\begin{cases} \dot{x} = t_{10}x + t_{11}xy + t_{20}x^2 + t_{02}y^2 + t_{30}x^3 + t_{21}x^2y + t_{12}xy^2 + t_{03}y^3 + P_7(x, y), \\ \dot{y} = p_{11}xy + p_{02}y^2 + p_{20}x^2y + p_{12}xy^2 + p_{03}y^3 + Q_7(x, y), \end{cases} \tag{2.16}$$

where

$$t_{10} = i_{10}, \quad t_{11} = i_{11} - \tfrac{2i_{20}i_{21}}{i_{10}} + \tfrac{i_{01}^2j_{11}}{i_{10}}, \quad t_{20} = \tfrac{i_{20}}{i_{10}}, \quad t_{02} = -i_{11}i_{01} + \tfrac{i_{20}i_{01}^2}{i_{10}} - \tfrac{i_{01}^2j_{11}}{i_{10}}, \quad t_{30} = \tfrac{i_{30}}{i_{10}^2},$$
$$t_{21} = -\tfrac{3i_{30}i_{01}}{i_{10}^2} + \tfrac{i_{21}}{i_{10}} + \tfrac{i_{01}j_{21}}{i_{10}^2}, \quad t_{12} = \tfrac{3i_{30}i_{01}^2}{i_{10}^2} - \tfrac{2i_{21}i_{01}}{i_{10}} + i_{12} - \tfrac{2i_{01}^2j_{21}}{i_{10}^2} + \tfrac{i_{01}j_{12}}{i_{10}},$$
$$t_{03} = -\tfrac{i_{30}i_{01}^3}{i_{10}^2} + \tfrac{i_{21}i_{01}^2}{i_{10}} - i_{12}i_{01} + \tfrac{i_{01}^3j_{21}}{i_{10}^2} - \tfrac{i_{01}^2j_{12}}{i_{10}}, \quad p_{11} = \tfrac{j_{11}}{i_{10}}, \quad p_{02} = -\tfrac{j_{11}i_{01}}{i_{10}}, \quad p_{21} = \tfrac{j_{21}}{i_{10}^2},$$
$$p_{12} = -\tfrac{2j_{21}i_{01}}{i_{10}^2} + \tfrac{j_{12}}{i_{10}}, \quad p_{03} = \tfrac{j_{21}i_{01}^2}{i_{10}^2} - \tfrac{j_{12}i_{01}}{i_{10}},$$

and $P_7(x, y)$ and $Q_7(x, y)$ are C^∞ functions at least of order fourth in (x, y).

We import a new variable τ to the model (2.16) by $\tau = t_{10}t$. For formal simplicity, we still use t instead of τ. We have the standard form

$$\begin{cases} \dot{x} = x + \frac{t_{11}}{t_{10}}xy + \frac{t_{20}}{t_{10}}x^2 + \frac{t_{02}}{t_{10}}y^2 + \frac{t_{30}}{t_{10}}x^3 + \frac{t_{21}}{t_{10}}x^2y + \frac{t_{12}}{t_{10}}xy^2 + \frac{t_{03}}{t_{10}}y^3 + P_8(x, y), \\ \dot{y} = \frac{p_{11}}{t_{10}}xy + \frac{p_{02}}{t_{10}}y^2 + \frac{p_{20}}{t_{10}}x^2y + \frac{p_{12}}{t_{10}}xy^2 + \frac{p_{03}}{t_{10}}y^3 + Q_8(x, y), \end{cases} \tag{2.17}$$

where $P_8(x, y)$ and $Q_8(x, y)$ are C^∞ functions at least of order fourth in (x, y). Hence, we find that the coefficient of y^2 is $\frac{p_{02}}{t_{10}}$ for the second equation of the model (2.17), i.e., $i_{10} \neq 0$, $i_{01} \neq 0$ and $j_{11} \neq 0$, then E_{24} is a saddle-node from Theorem 7.1 in Chapter 2 in the paper [46]. □

2.3.3. Stability of the internal equilibra

Theorem 2.7. If $\tilde{C}_1 = -(J_{11}^* + J_{22}^*) > 0$ and $\tilde{C}_2 = J_{11}^*J_{22}^* - J_{12}^*J_{21}^* > 0$, then the internal equilibrium point E^* (if it exists) is stable.

Proof. The Jacobian matrix of E^* is:

$$J_{E^*} = \begin{pmatrix} J_{11}^* & J_{12}^* \\ J_{21}^* & J_{22}^* \end{pmatrix},$$

where

$$J_{11}^* = \tfrac{r(1-\frac{2x^*}{K})}{1+my^*} - \tfrac{\lambda y^*(a+by^*)}{(a+x^*+by^*)^2} - \tfrac{q_1e_1^2c_1}{(c_1e_1+c_2x^*)^2} - m_1, \quad J_{12}^* = -rx^*(1-\tfrac{x^*}{K})\tfrac{m}{(1+my^*)^2} - \tfrac{\lambda x(a+x^*)}{(a+x^*+by^*)^2},$$
$$J_{21}^* = \tfrac{\delta\lambda y(a+by^*)}{(a+x^*+by^*)^2}, \quad J_{22}^* = \tfrac{\delta\lambda x^*(a+x^*)}{(a+x^*+by^*)^2} - m_2 + \tfrac{\alpha}{(1+\beta y^*)^2}.$$

The characteristic equation of the matrix J_{E^*} can be written as:

$$\xi^2 + \tilde{C}_1\xi + \tilde{C}_2 = 0,$$

with $\tilde{C}_1 = -(J^*_{11}+J^*_{22}), \tilde{C}_2 = J^*_{11}J^*_{22}-J^*_{12}J^*_{21}$. According to Routh-Hurwitz criteria, if $\tilde{C}_1 > 0$ and $\tilde{C}_2 > 0$, the characteristic equation of the matrix J_{E^*} has negative real parts. Thus, the internal equilibrium point E^* is stable (if present). □

2.4. Bifurcation analysis

In order to explore the dynamic behaviors that the model can exhibit and analyze population growth coexistence modes, we studied the occurrence of transcritical bifurcation, saddle-node bifurcation, and Hopf bifurcation of parameter α. Moreover, we will probe the conditions for codimension two bifurcations in this section, such as Bogdanov-Takens bifurcation.

2.4.1. Transcritical bifurcation

Theorem 2.8. If $\frac{\delta\lambda(a+2b)}{(a+x_{24})^2}v_1 \neq (\frac{b\delta\lambda x_{24}}{(a+x_{24})^2} - \alpha\beta)v_2$, the model (1.2) undergoes a transcritical bifurcation at the equilibrium point $E_{24}(x_{24}, 0)$ when $\alpha = \alpha_{TC} = m_2 - \frac{\delta\lambda x_{24}}{a+x_{24}}$.

Proof. If $\alpha = \alpha_{TC} = m_2 - \frac{\delta\lambda x_{24}}{a+x_{24}}$, the Jacobian matrix at E_{24} can be written in the following form:

$$J_{E_{24}} = \begin{pmatrix} r(1-\frac{2x_{24}}{K}) - \frac{q_1e_1^2c_1}{(c_1e_1+c_2x_{24})^2} - m_1 & -mrx_{24}(1-\frac{x_{24}}{K}) \\ 0 & 0 \end{pmatrix}.$$

Then, we test whether the corresponding conditions for transcritical bifurcation are true by Sotomayor's theorem. Suppose the eigenvectors of matrices $J_{E_{24}}$ and J^T_{E24} for zero eigenvalue are V and W, respectively.

With simple calculations, we know that the eigenvectors V and W respectively meet the following conditions:

$$-\left[r(1-\tfrac{2x_{24}}{K}) - \tfrac{q_1e_1^2c_1}{(c_1e_1+c_2x_{24})^2} - m_1\right]v_1 + \left[-mrx_{24}(1-\tfrac{x_{24}}{K})\right]v_2 = 0,$$
$$\begin{pmatrix} w_1 \\ w_2 \end{pmatrix} = \begin{pmatrix} 0 \\ 1 \end{pmatrix}.$$

Further, by a simple calculation, we have

$$F_\alpha(E_{24};\alpha_{TC}) = \begin{pmatrix} 0 \\ \frac{y}{1+\beta y} \end{pmatrix}_{(E_{24};\alpha_{TC})} = \begin{pmatrix} 0 \\ 0 \end{pmatrix},$$

$$DF_\alpha(E_{24};\alpha_{TC})V = \begin{pmatrix} 0 & 0 \\ 0 & 1 \end{pmatrix}\begin{pmatrix} v_1 \\ v_2 \end{pmatrix} = \begin{pmatrix} 0 \\ v_2 \end{pmatrix},$$

$$\begin{aligned} D^2F(E_{24};\alpha_{TC})(V,V) &= \begin{pmatrix} \frac{\partial^2F_1}{\partial x^2}v_1v_1 + 2\frac{\partial^2F_1}{\partial x\partial y}v_1v_2 + \frac{\partial^2F_1}{\partial y^2}v_2v_2 \\ \frac{\partial^2F_2}{\partial x^2}v_1v_1 + 2\frac{\partial^2F_2}{\partial x\partial y}v_1v_2 + \frac{\partial^2F_2}{\partial y^2}v_2v_2 \end{pmatrix}_{(E_{24};\alpha_{TC})} \\ &= \begin{pmatrix} \left[-\frac{2r}{K} + \frac{2q_1e_1^2c_1c_2}{(c_1e_1+c_2x_{24})^3}\right]v_1^2 + 2\left[mr(\frac{2x_{24}}{K}-1) - \frac{\lambda a}{(a+x_{24})^2}\right]v_1v_2 + \left[2m^2rx_{24}(1-\frac{x_{24}}{K}) + 2\frac{\lambda bx_{24}}{(a+x_{24})^2}\right]v_2^2 \\ 2\frac{\delta\lambda(a+2b)}{(a+x_{24})^2}v_1v_2 + \left[-2\frac{b\delta\lambda x_{24}}{(a+x_{24})^2} - 2\alpha\beta\right]v_2^2 \end{pmatrix}. \end{aligned}$$

Therefore, we verify the following conditions:

$$W^T F_\alpha(E_{24};\alpha_{TC}) = \begin{pmatrix}0 & 1\end{pmatrix}\begin{pmatrix}0\\0\end{pmatrix} = 0,$$

$$W^T\left[DF_\alpha(E_{24};\alpha_{TC})V\right] = \begin{pmatrix}0 & 1\end{pmatrix}\begin{pmatrix}0\\v_2\end{pmatrix} = v_2 \neq 0,$$

$$W^T\left[D^2F_\alpha(E_{24};\alpha_{TC})(V,V)\right] = 2v_2\left[\tfrac{\delta\lambda(a+2b)}{(a+x_{24})^2}v_1 - (\tfrac{b\delta\lambda x_{24}}{(a+x_{24})^2} - \alpha\beta)v_2\right] \neq 0.$$

Hence, if $\alpha = \alpha_{TC} = m_2 - \frac{\delta\lambda x_{24}}{a+x_{24}}$, the model (1.2) will experience a transcritical bifurcation at E_{24}. □

2.4.2. Saddle-node bifurcation

Saddle-node bifurcation is the convergence of two equilibrium points with different stability characteristics and no longer exist, resulting in a local bifurcation of a saddle-node at the point where they collide. Since there is no explicit expression for the components of the internal equilibrium point, the occurrence of saddle-node bifurcation can only be expressed numerically. For the parameter values in Table 2, we observe that the model (1.2) has a saddle-node bifurcation at threshold $\alpha_{SN} = 0.2227608967$, around the coincident equilibriun point $E_+ = (x_+, y_+) = (1.601447995, 1.0727568325)$.

Then, we check whether the corresponding condition for saddle-node bifurcation holds true by Sotomayor's theorem again. First, if $\alpha = \alpha_{SN}$, the Jacobian matrix of E_+ can be written in the following form:

$$J_{E_+} = \begin{pmatrix}0.0983189543 & -0.3439189244\\0.01223578181 & -0.0428006681\end{pmatrix}.$$

Obviously, one of the eigenvalues of the matrix J_{E_+} is zero. Suppose the eigenvector of the zero eigenvalue of the matrix J_{E_+} and $J^T_{E_+}$ are V and W, then

$$V = \begin{pmatrix}v_1\\v_2\end{pmatrix} = \begin{pmatrix}0.123497203413162\\0.274866912334495\end{pmatrix}, \quad W = \begin{pmatrix}w_1\\w_2\end{pmatrix} = \begin{pmatrix}-0.961482282990020\\0.992344920251587\end{pmatrix}.$$

Therefore, we have

$$F_\alpha(E_+;\alpha_{SN}) = \begin{pmatrix}0\\\frac{y}{1+\beta y}\end{pmatrix}_{(E_+;\alpha_{SN})} = \begin{pmatrix}0\\0.8115712506\end{pmatrix},$$

$$D^2F(E_+;\alpha_{SN})(V,V) = \begin{pmatrix}\frac{\partial^2F_1}{\partial x^2}v_1v_1 + 2\frac{\partial^2F_1}{\partial x\partial y}v_1v_2 + \frac{\partial^2F_1}{\partial y^2}v_2v_2\\\frac{\partial^2F_2}{\partial x^2}v_1v_1 + 2\frac{\partial^2F_2}{\partial x\partial y}v_1v_2 + \frac{\partial^2F_2}{\partial y^2}v_2v_2\end{pmatrix}_{(E_+;\alpha_{TSN})} = \begin{pmatrix}-0.005807048836\\-0.003953245102\end{pmatrix}.$$

Finally, we have

$$W^T F_\alpha(E_+;\alpha_{SN}) = 0.8053586080 \neq 0,$$

$$W^T\left[D^2F_\alpha(E_+;\alpha_{SN})(V,V)\right] = 0.001660391876 \neq 0.$$

Hence, the model (1.2) experiences a saddle-node bifurcation when the parameter α satisfies the condition $\alpha = \alpha_{SN}$.

2.4.3. Hopf bifurcation

Through numerical analysis, we know that E_1^* is always a saddle whenever it exists, and the internal equilibrium point E_2^* is locally asymptotically stable under certain conditions. Therefore, E_2^* are potential susceptibility to Hopf bifurcation. We specify α as the variable that may cause Hopf bifurcation, which is derived from the condition that the trace is equal to zero. When α changes and exceeds the threshold α_H, the stability of E_2^* is disrupted. Subsequently, we will provide a rigorous piece of evidence to support this conclusion.

Theorem 2.9. If $\tilde{C}_1(\alpha_H) = 0$ and $\tilde{C}_2(\alpha_H) > 0$, in the vicinity of the internal equilibrium point E_2^*, the model (1.2) undergoes a Hopf bifurcation at the critical values α, $\alpha = \alpha_H$.

Proof. According to Theorem 2.7, we get the characteristic equation of the matrix $J_{E_2^*}$:

$$\xi^2 + \tilde{C}_1\xi + \tilde{C}_2 = 0.$$

Next, we have obtained that $Tr(J_{E_2^*}) = \tilde{C}_1(\alpha_H) = 0$ and $Det(J_{E_2^*}) = \tilde{C}_2(\alpha_H) > 0$ when $\alpha = \alpha_H$. Therefore, we only need to check the correctness of the cross-sectional condition of the Hopf bifurcation. That is,

$$\frac{\mathrm{d}Re(\xi)}{\mathrm{d}\alpha}\Big|_{\alpha=\alpha_H} \neq 0,$$

and the solution of the characteristic equation can be written as

$$\xi_1 = -\frac{\tilde{C}_1}{2} + i\frac{\sqrt{4\tilde{C}_2 - \tilde{C}_1^{\,2}}}{2}, \quad \xi_2 = -\frac{\tilde{C}_1}{2} - i\frac{\sqrt{4\tilde{C}_2 - \tilde{C}_1^{\,2}}}{2}.$$

Let $u = -\frac{\tilde{C}_1}{2}$, $v = \frac{\sqrt{4\tilde{C}_2 - \tilde{C}_1^{\,2}}}{2}$, and the solution of the characteristic equation can be written as

$$\xi_1 = u + iv, \quad \xi_2 = u - iv.$$

Substitute the above roots into the equation to separate the real part and the imaginary part, and we can obtain,

$$\begin{cases} u^2 - v^2 + \tilde{C}_1 u + \tilde{C}_2 = 0, \\ 2uv + \tilde{C}_1 v = 0. \end{cases}$$

From the Hopf bifurcation theorem, we know that ξ is the eigenvalue of a pure imaginary number. So, $u(\alpha_H) = 0$ and $v(\alpha_H) \neq 0$, and the equations can be written as

$$\begin{cases} -v^2(\alpha_H) + \tilde{C}_2(\alpha_H) = 0, \\ \tilde{C}_1(\alpha_H)v(\alpha_H) = 0. \end{cases}$$

Thus, we can get $\tilde{C}_1(\alpha_H) = 0$ and $\tilde{C}_2(\alpha_H) = v^2(\alpha_H)$. On differentiating the equation with respect to α and putting $\alpha = \alpha_H$, we get

$$\begin{cases} -2v(\alpha_H)\frac{\mathrm{d}v}{\mathrm{d}\alpha}|_{\alpha=\alpha_H} + \frac{\mathrm{d}\tilde{C}_2}{\mathrm{d}\alpha}|_{\alpha=\alpha_H} = 0, \\ 2v(\alpha_H)\frac{\mathrm{d}u}{\mathrm{d}\alpha}|_{\alpha=\alpha_H} + v(\alpha_H)\frac{\mathrm{d}\tilde{C}_1}{\mathrm{d}\alpha}|_{\alpha=\alpha_H} = 0. \end{cases}$$

Compute $\frac{\mathrm{d}Re(\xi)}{\mathrm{d}\alpha}|_{\alpha=\alpha_H}$ from the above equations, and we get

$$\left.\frac{\mathrm{d}Re(\xi)}{\mathrm{d}\alpha}\right|_{\alpha=\alpha_H} = \left.\frac{\mathrm{d}u}{\mathrm{d}\alpha}\right|_{\alpha=\alpha_H} = \frac{-\left.\frac{\mathrm{d}\bar{C}_1}{\mathrm{d}\alpha}\right|_{\alpha=\alpha_H}}{2} = -\frac{1}{2(1+\beta y_2^*)^2} \neq 0.$$

Therefore, the transversal condition holds. Thus, the model (1.2) exhibits a Hopf bifurcation around the equilibrium point E_2^* at $\alpha = \alpha_H$.

It is necessary to determine the orientation and stability of the limit cycle, and then we will calculate the Lyapunov number.

Convert E_2^* to the origin by transforming $p = x - x_2^*$, $q = y - y_2^*$, therefore, the model (1.2) in the origin region is shown below

$$\begin{cases} \dot{p} = e_{10}p + e_{01}q + e_{11}pq + e_{20}p^2 + e_{02}q^2 + e_{30}p^3 + e_{21}p^2q + e_{12}pq^2 + e_{03}q^3 + P_{10}(p,q), \\ \dot{q} = f_{10}p + f_{01}q + f_{11}pq + f_{20}p^2 + f_{02}q^2 + f_{30}p^3 + f_{21}p^2q + f_{12}pq^2 + f_{03}q^3 + Q_{10}(p,q), \end{cases} \tag{2.18}$$

where

$$\begin{aligned}
e_{10} &= \frac{r(K-2x_2^*)}{K\left(my_2^*+1\right)} - \frac{\lambda y_2^*(a+by_2^*)}{\left(by_2^*+a+x_2^*\right)^2} - \frac{q_1e_1^2c_1}{\left(c_2x_2^*+c_1e_1\right)^2} - m_1, \quad e_{01} = -\frac{rx_2^*\left(K-x_2^*\right)m}{K\left(my_2^*+1\right)^2} - \frac{\lambda x_2^*(a+x_2^*)}{\left(by_2^*+a+x_2^*\right)^2}, \\
e_{11} &= -\frac{rm(K-2x_2^*)}{K\left(my_2^*+1\right)^2} - \frac{a\lambda(by_2^*+a+x_2^*)+2\lambda x_2^*y_2^*b}{\left(by_2^*+a+x_2^*\right)^3}, \quad e_{20} = -\frac{r}{\left(my_2^*+1\right)K} + \frac{\lambda y_2^*(a+by_2^*)}{\left(by_2^*+a+x_2^*\right)^3} + \frac{e_1^2q_1c_1c_2}{\left(c_1e_1+c_2x_2^*\right)^3}, \\
e_{02} &= \frac{rx_2^*\left(K-x_2^*\right)m^2}{K\left(my_2^*+1\right)^3} + \frac{\lambda x_2^*b(a+x_2^*)}{\left(by_2^*+a+x_2^*\right)^3}, \quad e_{30} = -\frac{\lambda y_2^*(a+by_2^*)}{\left(by_2^*+a+x_2^*\right)^4} - \frac{e_1^2q_1c_1c_2^2}{\left(c_1e_1+c_2x_2^*\right)^4}, \\
e_{21} &= \frac{rm}{K\left(my_2^*+1\right)^2} + \frac{\lambda\left[-b^2y_2^{*2}+2bx_2^*y_2^*+a(a+x_2^*)\right]}{\left(by_2^*+a+x_2^*\right)^4}, \quad e_{12} = \frac{r\left(K-2x_2^*\right)m^2}{K\left(my_2^*+1\right)^3} + \frac{\lambda b\left[by_2^*(a+2x_2^*)+a^2-x_2^{*2}\right]}{\left(by_2^*+a+x_2^*\right)^4}, \\
e_{03} &= -\frac{rx_2^*\left(K-x_2^*\right)m^3}{K\left(my_2^*+1\right)^4} - \frac{\lambda x_2^*b^2(a+x_2^*)}{\left(by_2^*+a+x_2^*\right)^4}, \quad f_{10} = \frac{\delta\lambda y_2^*(a+by_2^*)}{\left(by_2^*+a+x_2^*\right)^2}, \quad f_{01} = \frac{\delta\lambda x_2^*(a+x_2^*)}{\left(by_2^*+a+x_2^*\right)^2} - m_2 + \frac{\alpha}{\left(\beta y_2^*+1\right)^2}, \\
f_{11} &= \frac{\delta\lambda\left[a^2+a(x_2^*+by_2^*)+2bx_2^*y_2^*\right]}{\left(by_2^*+a+x_2^*\right)^3}, \quad f_{20} = -\frac{\delta\lambda y_2^*(a+by_2^*)}{(a+x_2^*+by_2^*)^3}, \quad f_{02} = -\frac{\delta\lambda bx_2^*(a+x_2^*)}{\left(by_2^*+a+x_2^*\right)^3} - \frac{\alpha\beta}{\left(\beta y_2^*+1\right)^3}, \\
f_{30} &= \frac{\delta\lambda y_2^*(a+by_2^*)}{\left(by_2^*+a+x_2^*\right)^4}, \quad f_{21} = -\frac{\delta\lambda\left[(a+by_2^*)(a-by_2^*)+x_2^*(a+2by_2^*)\right]}{\left(by_2^*+a+x_2^*\right)^4}, \quad f_{12} = -\frac{\delta\lambda b\left(aby_2^*+2x_2^*y_2^*b+a^2-x_2^{*2}\right)}{\left(by_2^*+a+x_2^*\right)^4}, \\
f_{03} &= \frac{\delta\lambda\, b^2x_2^*(a+x_2^*)}{\left(by_2^*+a+x_2^*\right)^4} + \frac{\alpha\beta^2}{\left(\beta y_2^*+1\right)^4},
\end{aligned}$$

and $P_{10}(p,q)$, $Q_{10}(p,q)$ are C^∞ functions at least of order fourth in (p,q).

The first Lyapunov number is

$$\begin{aligned}
l_1 = \frac{-3\pi}{2e_{01}Det^{\frac{3}{2}}} \Big\{ &\Big[e_{10}f_{10}(e_{11}^2 + e_{11}f_{02} + e_{02}f_{11}) + e_{10}e_{01}(f_{11}^2 + e_{20}f_{11} + e_{11}f_{02}) + f_{10}^2(e_{11}e_{02} + 2e_{02}f_{02}) \\
&-2e_{10}f_{10}(f_{02}^2 - e_{20}e_{02}) - 2e_{10}e_{01}(e_{20}^2 - f_{20}f_{02}) - e_{01}^2(2e_{20}f_{20} + f_{11}f_{20}) + (e_{01}f_{10-2e_{10}^2})(f_{11}f_{02} - e_{11}e_{20})\Big] \\
&-(e_{10}^2 + e_{01}f_{10})\left[3(f_{10}f_{03} - e_{01}e_{30}) + 2e_{10}(e_{21} + f_{12}) + (e_{12}f_{10} - e_{01}f_{20})\right]\Big\}.
\end{aligned}$$

From Theorem 1 of Section 4.4 of the paper [47], we draw the following conclusions. When $l_1 > 0$, the limit cycle around E_2^* is unstable and the Hopf bifurcation is subcritical. When $l_1 < 0$, the limit cycle around E_2^* is stable, and E_2^* loses its stability due to a supercritical Hopf bifurcation.

Because the formula of the first Lyapunov number l_1 is too complicated, we cannot easily determine its sign. Therefore, the rationality of the Theorem 2.9 will be verified in the next simulation. □

2.4.4. Bogdanov-Takens bifurcation

Above we discussed the bifurcation of codimension one at the nonhyperbolic equilibrium point, and next we will prove the possibility of Bogdanov-Takens bifurcation of codimension 2. Earlier, we know that y_+ is a dual positive root, and when some conditions are satisfied, E_+ is a cusp of codimension 2. Next, we will explore the Bogdanov-Takens bifurcation with the parameters α and λ.

Theorem 2.10. If we choose bifurcation parameters α and λ, then the model (1.2) experiences a Bogdanov-Takens bifurcation around E_+ with changing parameters (α, λ) near $(\alpha_{BT}, \lambda_{BT})$. $(\alpha_{BT}, \lambda_{BT})$ denotes the bifurcation threshold value, i.e.,

$$Det(J_{E_+})|_{(\alpha_{BT},\lambda_{BT})} = 0, \quad Tr(J_{E_+})|_{(\alpha_{BT},\lambda_{BT})} = 0.$$

Proof. In order to obtain the exact expressions of saddle-nodes, Hopf and homoclinic bifurcation curve for small neighborhoods near the Bogdanov-Takens point, we convert the model (1.2) into the standard form of the Bogdanov-Takens bifurcation.

Then, parameter vectors $(\varepsilon_1, \varepsilon_2)$ are introduced near $(0, 0)$ in order to perturb α and λ near the Bogdanov-Takens bifurcation values given by $\alpha = \alpha_{BT} + \varepsilon_1$ and $\lambda = \lambda_{BT} + \varepsilon_2$. Substituting the perturbation into the model (1.2), we get

$$\begin{cases} \dfrac{\mathrm{d}x}{\mathrm{d}t} = rx(1 - \dfrac{x}{K})\dfrac{1}{1+my} - \dfrac{(\lambda+\varepsilon_1)xy}{a+x+by} - \dfrac{q_1e_1x}{c_1e_1+c_2x} - m_1x, \\ \dfrac{\mathrm{d}y}{\mathrm{d}t} = \dfrac{\delta(\lambda+\varepsilon_1)xy}{a+x+by} + \dfrac{(\alpha+\varepsilon_2)y}{1+\beta y} - m_2y. \end{cases} \tag{2.19}$$

Let $(0, 0)$ become the bifurcation point by introducing the transformation $\Upsilon_1 = x - x_+$, $\Upsilon_2 = y - y_+$, and we get

$$\begin{cases} \dfrac{\mathrm{d}\Upsilon_1}{\mathrm{d}t} = m_{00}(\varepsilon) + m_{10}(\varepsilon)\Upsilon_1 + m_{01}(\varepsilon)\Upsilon_2 + m_{11}(\varepsilon)\Upsilon_1\Upsilon_2 + m_{20}(\varepsilon)\Upsilon_1^2 + m_{02}(\varepsilon)\Upsilon_2^2 + P_1(\Upsilon_1, \Upsilon_2, \varepsilon), \\ \dfrac{\mathrm{d}\Upsilon_2}{\mathrm{d}t} = n_{00}(\varepsilon) + n_{10}(\varepsilon)\Upsilon_1 + n_{01}(\varepsilon)\Upsilon_2 + n_{11}(\varepsilon)\Upsilon_1\Upsilon_2 + n_{20}(\varepsilon)\Upsilon_1^2 + n_{02}(\varepsilon)\Upsilon_2^2 + Q_1(\Upsilon_1, \Upsilon_2, \varepsilon), \end{cases} \tag{2.20}$$

where

$$\begin{aligned}
&m_{00} = \tfrac{rx_+(K-x_+)}{K(1+my_+)} - \tfrac{(\lambda+\varepsilon_1)x_+y_+}{a+x_++by_+} - \tfrac{q_1e_1x_+}{c_1e_1+c_2x_+} - m_1x_+, \quad m_{10} = \tfrac{r(K-2x_+)}{K(my_++1)} - \tfrac{(\lambda+\varepsilon_1)y_+(a+by_+)}{(by_++a+x_+)^2} - \tfrac{q_1e_1^2c_1}{(c_2x_++c_1e_1)^2} - m_1, \\
&m_{01} = -\tfrac{rx_+(K-x_+)m}{K(my_++1)^2} - \tfrac{(\lambda+\varepsilon_1)x_+(a+x_+)}{(by_++a+x_+)^2}, \quad m_{11} = -\tfrac{rm(K-2x_+)}{K(my_++1)^2} - \tfrac{a(\lambda+\varepsilon_1)(by_++a+x_+)+2(\lambda+\varepsilon_1)x_+y_+b}{(by_++a+x_+)^3}, \\
&m_{20} = -\tfrac{r}{(my_++1)K} + \tfrac{(\lambda+\varepsilon_1)y_+(a+by_+)}{(by_++a+x_+)^3} + \tfrac{e_1^2q_1c_1c_2}{(c_1e_1+c_2x_+)^3}, \quad m_{02} = \tfrac{rx_+(K-x_+)m^2}{K(my_++1)^3} + \tfrac{(\lambda+\varepsilon_1)x_+b(a+x_+)}{(by_++a+x_+)^3}, \\
&n_{00} = \tfrac{\delta(\lambda+\varepsilon_1)x_+y_+}{a+x_++by_+} + \tfrac{(\alpha+\varepsilon_2)y_+}{1+\beta y_+} - m_2y_+, \quad n_{10} = \tfrac{\delta(\lambda+\varepsilon_1)y_+(a+by_+)}{(by_++a+x_+)^2}, \quad n_{01} = \tfrac{\delta(\lambda+\varepsilon_1)x_+(a+x_+)}{(by_++a+x_+)^2} - m_2 + \tfrac{\alpha+\varepsilon_2}{(\beta y_++1)^2}, \\
&n_{11} = \tfrac{\delta(\lambda+\varepsilon_1)\left[a^2+a(x_++by_+)+2bx_+y_+\right]}{(by_++a+x_+)^3}, \quad n_{20} = -\tfrac{\delta\lambda y_+(a+by_+)}{(a+x_++by_+)^3}, \quad n_{02} = -\tfrac{\delta(\lambda+\varepsilon_1)bx_+(a+x_+)}{(by_++a+x_+)^3} - \tfrac{(\alpha+\varepsilon_2)\beta}{(\beta y_++1)^3},
\end{aligned}$$

and $P_1(\Upsilon_1, \Upsilon_2, \varepsilon)$, $Q_1(\Upsilon_1, \Upsilon_2, \varepsilon)$ is the power series in (Υ_1, Υ_2) with terms $\Upsilon_1^i\Upsilon_2^j$ requiring $i + j \geq 3$, their coefficients depending on ε_1 and ε_2 smoothly.

In the following, we perform the transformation

$$X = \Upsilon_1, \quad Y = m_{10}(\varepsilon)\Upsilon_1 + m_{01}(\varepsilon)\Upsilon_2,$$

and model (2.20) becomes

$$\begin{cases} \dfrac{\mathrm{d}X}{\mathrm{d}t} = i_{00}(\varepsilon) + Y + i_{20}(\varepsilon)X^2 + i_{11}(\varepsilon)XY + i_{02}(\varepsilon)Y^2 + P_2(X, Y, \varepsilon), \\ \dfrac{\mathrm{d}Y}{\mathrm{d}t} = j_{00}(\varepsilon) + j_{10}(\varepsilon)X + j_{01}(\varepsilon)Y + j_{20}(\varepsilon)X^2 + j_{11}(\varepsilon)XY + j_{02}(\varepsilon)Y^2 + Q_2(X, Y, \varepsilon), \end{cases} \tag{2.21}$$

where

$$\begin{aligned} &i_{00}(\varepsilon) = m_{00}(\varepsilon), \quad i_{20}(\varepsilon) = \tfrac{m_{01}^2(\varepsilon)m_{20}(\varepsilon) - m_{11}(\varepsilon)m_{10}(\varepsilon)m_{01}(\varepsilon) + m_{02}(\varepsilon)m_{10}^2(\varepsilon)}{m_{01}^2(\varepsilon)}, \quad i_{11}(\varepsilon) = \tfrac{m_{01}(\varepsilon)m_{11}(\varepsilon) - 2m_{02}(\varepsilon)m_{10}(\varepsilon)}{m_{01}^2(\varepsilon)}, \\ &i_{02}(\varepsilon) = \tfrac{m_{02}(\varepsilon)}{m_{01}^2(\varepsilon)}, \quad j_{00}(\varepsilon) = m_{00}(\varepsilon)m_{10}(\varepsilon) + n_{00}(\varepsilon)m_{01}(\varepsilon), \quad j_{10}(\varepsilon) = n_{10}(\varepsilon)m_{01}(\varepsilon) - n_{01}(\varepsilon)m_{10}(\varepsilon), \\ &j_{01}(\varepsilon) = m_{10}(\varepsilon) + n_{01}(\varepsilon), \\ &j_{20}(\varepsilon) = \tfrac{m_{01}^3(\varepsilon)n_{20}(\varepsilon) - m_{01}(\varepsilon)m_{10}^2(\varepsilon)m_{11}(\varepsilon) + m_{01}(\varepsilon)m_{10}^2(\varepsilon)n_{02}(\varepsilon) + m_{02}(\varepsilon)m_{10}^3(\varepsilon)}{m_{01}^2(\varepsilon)} + m_{10}(\varepsilon)m_{20}(\varepsilon) - m_{10}(\varepsilon)n_{11}(\varepsilon), \\ &j_{11}(\varepsilon) = \tfrac{m_{01}^2(\varepsilon)n_{11}(\varepsilon) + m_{11}(\varepsilon)m_{10}(\varepsilon)m_{01}(\varepsilon) - 2m_{01}(\varepsilon)m_{10}(\varepsilon)n_{02}(\varepsilon) - 2m_{02}(\varepsilon)m_{10}^2(\varepsilon)}{m_{01}^2(\varepsilon)}, \quad j_{02}(\varepsilon) = \tfrac{n_{02}(\varepsilon)m_{01}(\varepsilon) + m_{02}(\varepsilon)m_{10}(\varepsilon)}{m_{01}^2(\varepsilon)}, \end{aligned}$$

and $P_2(X, Y, \varepsilon)$, $Q_2(X, Y, \varepsilon)$ is the power series in (X, Y) with terms X^iY^j requiring $i + j \geq 3$, their coefficients depending on ε_1 and ε_2 smoothly.

Then introducing the next C^∞ change of coordinates in a small domain of $(0, 0)$:

$$\theta_1 = X, \quad \theta_2 = i_{00}(\varepsilon) + Y + i_{20}(\varepsilon)X^2 + i_{11}(\varepsilon)XY + i_{02}(\varepsilon)Y^2 + P_2(X, Y, \varepsilon),$$

the model (2.21) can be written as

$$\begin{cases} \dfrac{\mathrm{d}\theta_1}{\mathrm{d}t} = \theta_2, \\ \dfrac{\mathrm{d}\theta_2}{\mathrm{d}t} = w_{00}(\varepsilon) + w_{10}(\varepsilon)\theta_1 + w_{01}(\varepsilon)\theta_2 + w_{20}(\varepsilon)\theta_1^2 + w_{11}(\varepsilon)\theta_1\theta_2 + w_{02}(\varepsilon)\theta_2^2 + Q_3(\theta_1, \theta_2, \varepsilon), \end{cases} \tag{2.22}$$

where

$$\begin{aligned} w_{00}(\varepsilon) &= j_{00}(\varepsilon) - i_{00}(\varepsilon)j_{01}(\varepsilon) + i_{00}^2(\varepsilon)j_{02}(\varepsilon) - 2i_{00}(\varepsilon)i_{02}(\varepsilon)j_{00}(\varepsilon) + \cdots, \\ w_{10}(\varepsilon) &= j_{10}(\varepsilon) + i_{11}(\varepsilon)j_{00}(\varepsilon) - i_{00}(\varepsilon)j_{11}(\varepsilon) - 2i_{00}(\varepsilon)i_{02}(\varepsilon)j_{10}(\varepsilon) + \cdots, \\ w_{01}(\varepsilon) &= j_{01}(\varepsilon) + 2i_{02}(\varepsilon)j_{00}(\varepsilon) - 2i_{00}(\varepsilon)j_{02}(\varepsilon) - i_{00}(\varepsilon)i_{11}(\varepsilon) - 4i_{00}(\varepsilon)i_{02}(\varepsilon)j_{01}(\varepsilon) + \cdots, \\ w_{20}(\varepsilon) &= j_{20}(\varepsilon) - i_{20}(\varepsilon)j_{01}(\varepsilon) + i_{11}(\varepsilon)j_{10}(\varepsilon) - 2i_{02}(\varepsilon)i_{20}(\varepsilon)j_{00}(\varepsilon) + 2i_{00}(\varepsilon)i_{20}(\varepsilon)j_{02}(\varepsilon) \\ &\quad -2i_{00}(\varepsilon)i_{02}(\varepsilon)j_{20}(\varepsilon) + \cdots, \\ w_{11}(\varepsilon) &= j_{11}(\varepsilon) + 2i_{20}(\varepsilon) + 2i_{02}(\varepsilon)j_{10}(\varepsilon) - 2i_{02}(\varepsilon)i_{11}(\varepsilon)j_{00}(\varepsilon) + 2i_{00}(\varepsilon)i_{11}(\varepsilon)j_{02}(\varepsilon) + i_{00}(\varepsilon)i_{11}^2(\varepsilon) \\ &\quad -4i_{00}(\varepsilon)i_{02}(\varepsilon)j_{11}(\varepsilon) + \cdots, \\ w_{02}(\varepsilon) &= j_{02}(\varepsilon) + i_{11}(\varepsilon) + 2i_{02}(\varepsilon)j_{01}(\varepsilon) + \cdots, \end{aligned}$$

and $Q_3(\theta_1, \theta_2, \varepsilon)$ is the power series in (θ_1, θ_2) with terms $\theta_1^i\theta_2^j$ requiring $i + j \geq 3$, their coefficients depending on ε_1 and ε_2 smoothly.

Use a new variable τ by $dt = (1 - w_{02}(\varepsilon)\theta_1)d\tau$, then we have

$$\begin{cases} \frac{\mathrm{d}\theta_1}{\mathrm{d}\tau} = \theta_2(1 - w_{02}(\varepsilon)\theta_1), \\ \frac{\mathrm{d}\theta_2}{\mathrm{d}\tau} = (1 - w_{02}(\varepsilon)\theta_1)\Big[w_{00}(\varepsilon) + w_{10}(\varepsilon)\theta_1 + w_{01}(\varepsilon)\theta_2 + w_{20}(\varepsilon)\theta_1^2 + w_{11}(\varepsilon)\theta_1\theta_2 + w_{02}(\varepsilon)\theta_2^2 + Q_3(\theta_1, \theta_2, \varepsilon)\Big]. \end{cases} \tag{2.23}$$

Let

$$\eta_1 = \theta_1, \quad \eta_2 = \theta_2(1 - w_{02}(\varepsilon)\theta_1),$$

then the model (2.23) can be rewritten as

$$\begin{cases} \dfrac{\mathrm{d}\eta_1}{\mathrm{d}\tau} = \eta_2, \\ \dfrac{\mathrm{d}\eta_2}{\mathrm{d}\tau} = g_{00}(\varepsilon) + g_{10}(\varepsilon)\eta_1 + g_{01}(\varepsilon)\eta_2 + g_{11}(\varepsilon)\eta_1\eta_2 + g_{20}(\varepsilon)\eta_1^2 + Q_4(\eta_1, \eta_2, \varepsilon), \end{cases} \tag{2.24}$$

where

$$\begin{aligned} &g_{00}(\varepsilon) = w_{00}(\varepsilon), \quad g_{10}(\varepsilon) = w_{10}(\varepsilon) - 2w_{00}(\varepsilon)w_{02}(\varepsilon), \quad g_{01}(\varepsilon) = w_{01}(\varepsilon), \\ &g_{11}(\varepsilon) = w_{11}(\varepsilon) - w_{01}(\varepsilon)w_{02}(\varepsilon), \quad g_{20}(\varepsilon) = w_{20}(\varepsilon) + w_{00}(\varepsilon)w_{02}^2(\varepsilon) - 2w_{02}(\varepsilon)w_{10}(\varepsilon), \end{aligned}$$

and $Q_4(\eta_1, \eta_2, \varepsilon)$ is a power series in (η_1, η_2) with terms $\eta_1^i\eta_2^j$ requiring $i + j \geq 3$, their coefficients depending on ε_1 and ε_2 smoothly.

We note that $g_{20}(\varepsilon)$ is a very complex number, so when ε_1 and ε_2 are small enough, it is difficult to discern the sign of $g_{20}(\varepsilon)$. So, for the next transformation to be meaningful, we must move on to the next two cases.

Case1: For ε_1 and ε_2 which are small enough, if $g_{20}(\varepsilon) > 0$, then we use the next transform:

$$\chi_1 = \eta_1, \quad \chi_2 = \frac{\eta_2}{\sqrt{g_{20}(\varepsilon)}}, \quad T = \sqrt{g_{20}(\varepsilon)}\tau,$$

and we get

$$\begin{cases} \dfrac{\mathrm{d}\chi_1}{\mathrm{d}T} = \chi_2, \\ \dfrac{\mathrm{d}\chi_2}{\mathrm{d}T} = M_{00}(\varepsilon) + M_{10}(\varepsilon)\chi_1 + M_{01}(\varepsilon)\chi_2 + M_{11}(\varepsilon)\chi_1\chi_2 + \chi_1^2 + Q_5(\chi_1, \chi_2, \varepsilon), \end{cases} \tag{2.25}$$

where

$$M_{00}(\varepsilon) = \frac{g_{00}(\varepsilon)}{g_{20}(\varepsilon)}, \quad M_{10}(\varepsilon) = \frac{g_{10}(\varepsilon)}{g_{20}(\varepsilon)}, \quad M_{01}(\varepsilon) = \frac{g_{01}(\varepsilon)}{\sqrt{g_{20}(\varepsilon)}}, \quad M_{11}(\varepsilon) = \frac{g_{11}(\varepsilon)}{\sqrt{g_{20}(\varepsilon)}},$$

and $Q_5(\chi_1, \chi_2, \varepsilon)$ is a power series in (χ_1, χ_2) with terms $\chi_1^i\chi_2^j$ requiring $i + j \geq 3$, their coefficients depending on ε_1 and ε_2 smoothly.

Let

$$o_1 = \chi_1 + \frac{M_{10}(\varepsilon)}{2}, \quad o_2 = \chi_2,$$

then we can have

$$\begin{cases} \dfrac{\mathrm{d}o_1}{\mathrm{d}T} = o_2, \\ \dfrac{\mathrm{d}o_2}{\mathrm{d}T} = N_{00}(\varepsilon) + N_{01}(\varepsilon)o_2 + N_{11}(\varepsilon)o_1o_2 + o_1^2 + Q_6(o_1, o_2, \varepsilon), \end{cases} \tag{2.26}$$

where

$$N_{00}(\varepsilon) = M_{00}(\varepsilon) - \frac{1}{4}M_{10}^2(\varepsilon), \quad N_{01}(\varepsilon) = M_{01}(\varepsilon) - \frac{1}{2}M_{10}(\varepsilon)M_{11}(\varepsilon), \quad N_{11}(\varepsilon) = M_{11}(\varepsilon),$$

and $Q_6(o_1, o_2, \varepsilon)$ is a power series in (o_1, o_2) with terms $o_1^i o_2^j$ requiring $i + j \geq 3$, their coefficients depending on ε_1 and ε_2 smoothly.

Assume that $g_{11}(\varepsilon) \neq 0$, then$N_{11}(\varepsilon) = M_{11}(\varepsilon) = \frac{g_{11}(\varepsilon)}{\sqrt{g_{20}(\varepsilon)}} \neq 0$. Through the next transformation:

$$X = N_{11}^2(\varepsilon)o_1, \quad Y = N_{11}^3(\varepsilon)o_2, \quad t = \frac{1}{N_{11}(\varepsilon)}T,$$

then we can obtain

$$\begin{cases} \dfrac{\mathrm{d}X}{\mathrm{d}t} = Y, \\ \dfrac{\mathrm{d}Y}{\mathrm{d}t} = \varrho_1(\varepsilon) + \varrho_2(\varepsilon)Y + XY + X^2 + Q_7(X, Y, \varepsilon), \end{cases} \tag{2.27}$$

where

$$\varrho_1(\varepsilon) = N_{00}(\varepsilon)N_{11}^4(\varepsilon), \quad \varrho_2(\varepsilon) = N_{01}(\varepsilon)N_{11}(\varepsilon),$$

and $Q_7(X, Y, \varepsilon)$ is a power series in (X, Y) with terms $X^i Y^j$ requiring $i + j \geq 3$, their coefficients depending on ε_1 and ε_2 smoothly.

Case2: For ε_1 and ε_2 which are small enough, if $g_{20}(\varepsilon) < 0$, then we use the next transform:

$$\chi_1{}' = \eta_1, \quad \chi_2{}' = \frac{\eta_2}{\sqrt{-g_{20}(\varepsilon)}}, \quad T' = \sqrt{-g_{20}(\varepsilon)}\tau,$$

and we can get

$$\begin{cases} \dfrac{\mathrm{d}\chi_1{}'}{\mathrm{d}T'} = \chi_2{}', \\ \dfrac{\mathrm{d}\chi_2{}'}{\mathrm{d}T} = M_{00}{}'(\varepsilon) + M_{10}{}'(\varepsilon)\chi_1 + M_{01}{}'(\varepsilon)\chi_2{}' + M_{11}{}'(\varepsilon)\chi_1{}'\chi_2{}' + \chi_1{}'^2 + Q_5{}'(\chi_1{}', \chi_2{}', \varepsilon), \end{cases} \tag{2.28}$$

where

$$M_{00}{}'(\varepsilon) = -\frac{g_{00}(\varepsilon)}{g_{20}(\varepsilon)}, \quad M_{10}{}'(\varepsilon) = -\frac{g_{10}(\varepsilon)}{g_{20}(\varepsilon)}, \quad M_{01}{}'(\varepsilon) = \frac{g_{01}(\varepsilon)}{\sqrt{-g_{20}(\varepsilon)}}, \quad M_{11}{}'(\varepsilon) = \frac{g_{11}(\varepsilon)}{\sqrt{-g_{20}(\varepsilon)}},$$

and $Q_5{}'(\chi_1{}', \chi_2{}', \varepsilon)$ is power series in $(\chi_1{}', \chi_2{}')$ with terms $\chi_1{}'^i \chi_2{}'^j$ requiring $i + j \geq 3$, their coefficients depend on ε_1 and ε_2 smoothly.

Let

$$o_1{}' = \chi_1{}' + \frac{M_{10}{}'(\varepsilon)}{2}, \quad o_2{}' = \chi_2{}',$$

then we can get

$$\begin{cases} \dfrac{\mathrm{d}o_1{}'}{\mathrm{d}T'} = o_2{}', \\ \dfrac{\mathrm{d}o_2{}'}{\mathrm{d}T'} = N_{00}{}'(\varepsilon) + N_{01}{}'(\varepsilon)o_2{}' + N_{11}{}'(\varepsilon)o_1{}'o_2{}' + o_1{}'^2 + Q_6{}'(o_1{}', o_2{}', \varepsilon), \end{cases} \tag{2.29}$$

where

$$N_{00}{}'(\varepsilon) = M_{00}{}'(\varepsilon) - \frac{1}{4}M_{10}{}'^2(\varepsilon), \quad N_{01}{}'(\varepsilon) = M_{01}{}'(\varepsilon) - \frac{1}{2}M_{10}{}'(\varepsilon)M_{11}{}'(\varepsilon), \quad N_{11}{}'(\varepsilon) = M_{11}{}'(\varepsilon),$$

and $Q_6'(o_1', o_2', \varepsilon)$ is a power series in (o_1', o_2') with terms ${o_1'}^i {o_2'}^j$ requiring $i + j \geq 3$, their coefficients depending on ε_1 and ε_2 smoothly.

Assume that $g_{11}(\varepsilon) \neq 0$, then $N_{11}'(\varepsilon) = M_{11}'(\varepsilon) = \frac{g_{11}(\varepsilon)}{\sqrt{-g_{20}(\varepsilon)}} \neq 0$. Through the next transformation:

$$X' = {N_{11}'}^2(\varepsilon) o_1', \quad Y' = {N_{11}'}^3(\varepsilon) o_2', \quad t' = \frac{1}{N_{11}'(\varepsilon)} T',$$

then we can have

$$\begin{cases} \dfrac{\mathrm{d}X'}{\mathrm{d}t} = Y', \\ \dfrac{\mathrm{d}Y'}{\mathrm{d}t'} = \varrho_1'(\varepsilon) + \varrho_2'(\varepsilon) Y' + X'Y' + X'^2 + Q_7'(X', Y', \varepsilon), \end{cases} \tag{2.30}$$

where

$$\varrho_1'(\varepsilon) = N_{00}'(\varepsilon) {N_{11}'}^4(\varepsilon), \quad \varrho_2'(\varepsilon) = N_{01}'(\varepsilon) N_{11}'(\varepsilon),$$

and $Q_7'(X', Y', \varepsilon)$ is a power series in (X', Y') with terms ${X'}^i {Y'}^j$ requiring $i + j \geq 3$, their coefficients depending on ε_1 and ε_2 smoothly.

To reduce the number of cases to be considered, we have reserved $\varrho_1(\varepsilon)$ and $\varrho_2(\varepsilon)$ to stand for $\varrho_1'(\varepsilon)$ and $\varrho_2'(\varepsilon)$ in (2.30). If the matrix $\left|\frac{\partial(\varrho_1, \varrho_2)}{\partial(\varepsilon_1, \varepsilon_2)}\right|$ is nonsingular, then the transformation is a homomorphism in a sufficiently small domain of $(0, 0)$. Meanwhile, under the above condition, ϱ_1, ϱ_2 are two independent variables. From the conclusions in [47, 48] and [49], we can obtain that the Bogdanov-Takens bifurcation is produced when $\varepsilon = (\varepsilon_1, \varepsilon_2)$ is located at a fully small domain of $(0, 0)$. Therefore, the local formulas near the origin of the bifurcation curves can be written as ("+" denotes $g_{20}(\varepsilon) > 0$ and "−" denotes $g_{20}(\varepsilon) < 0$):

(1) The saddle-node bifurcation curve can be represented as

$$SN = \{(\varepsilon_1, \varepsilon_2) : \varrho_1(\varepsilon_1, \varepsilon_2) = 0, \varrho_2(\varepsilon_1, \varepsilon_2) \neq 0\};$$

(2) The Hopf bifurcation curve can be represented as

$$H = \left\{(\varepsilon_1, \varepsilon_2) : \varrho_1(\varepsilon_1, \varepsilon_2) < 0, \varrho_2(\varepsilon_1, \varepsilon_2) = \pm\sqrt{-\varrho_1(\varepsilon_1, \varepsilon_2)}\right\};$$

(3) The homoclinic bifurcation curve can be represented as

$$HL = \left\{(\varepsilon_1, \varepsilon_2) : \varrho_1(\varepsilon_1, \varepsilon_2) < 0, \varrho_2(\varepsilon_1, \varepsilon_2) = \pm\frac{5}{7}\sqrt{-\varrho_1(\varepsilon_1, \varepsilon_2)}\right\}.$$

Regarding the autonomous predator-prey model (1.2), the mathematical theory derivation work not only focused on population persistence, existence and stability of some equilibrium points in the model (1.2), but also analyzed in detail the specific bifurcation dynamic behaviors of the model (1.2), such as transcritical bifurcation, saddle-node bifurcation, Hopf bifurcation and Bogdanov-Takens bifurcation. These theoretical research results provided a theoretical basis for subsequent numerical simulation work, and qualitatively proved that bifurcation dynamics evolution can induce the formation of population growth coexistence modes.

3. The nonautonomous model

In the model (1.2), it is assumed that all parameters are independent of time. However, in the real world, the parameters in ecological models are not constant; instead, they change over time due to different ecological and environmental conditions. Therefore, we extend the autonomous model to a nonautonomous model by incorporating seasonal factors into some key parameters. In fact, we take the growth rate of predator population, the level of fear, and the harvesting effort of the prey population as time-dependent parameters, while the other parameters are assumed to be constant. Our main objective is to study the impact of seasonality in these ecological factors on the dynamics of the proposed predator-prey model. After considering the time dependence of the parameters m, e_1 and α, the model (1.2) is transformed into the following form:

$$\begin{cases} \frac{\mathrm{d}x}{\mathrm{d}t} = rx(1-\frac{x}{K})\frac{1}{1+m(t)y} - \frac{\lambda xy}{a+x+by} - \frac{q_1e_1(t)x}{c_1e_1(t)+c_2x} - m_1x, \\ \frac{\mathrm{d}y}{\mathrm{d}t} = \frac{\delta\lambda xy}{a+x+by} + \frac{\alpha(t)y}{1+\beta y} - m_2y. \end{cases} \tag{3.1}$$

A set of seasonally-forced parameters of the abovementioned system functions, namely $m(t)$, $e_1(t)$ and $\alpha(t)$, are all nonnegative, continuousm and bounded functions with a positive lower bound. In actual ecological systems, time-varying parameters are often not synchronized. Various ecological factors, such as environmental conditions, temperature and weather, can all lead to such changes. Although considering seasonal forcing parameters in different periods can better simulate real-world situations, it poses challenges to both mathematical analysis and numerical computation. In order to maintain traceability when we analyze the nonautonomous model(3.1), we simplify the assumption that all time-varying parameters share the same period. Although this assumption may deviate from the complexity of the real ecological dynamics, it enables us to effectively analyze the model (3.1) both mathematically and numerically.

Definition 3.1. For a continuous ω-periodic function $f(t)$ on $\mathbb{R}^+$, we define the following notations:

$$f^U = \sup_{t\in R} f(t), \quad f^l = \inf_{t\in R} f(t), \quad \bar{f} = \frac{1}{\omega}\int_0^\omega f(t)dt.$$

3.1. The boundedness of the solution

Theorem 3.1. The model (3.1) is bounded in R^2_+.

Proof. Obviously, we have

$$\begin{aligned} x(t) &= x(0)exp\left\{\int_0^t \left[r(1-\tfrac{x(\xi)}{K})\tfrac{1}{1+m(\xi)y(\xi)} - \tfrac{\lambda x(\xi)y(\xi)}{a+x(\xi)+by(\xi)} - \tfrac{q_1e_1(\xi)x(\xi)}{c_1e_1(\xi)+c_2x(\xi)} - m_1x(\xi)\right]\mathrm{d}\xi\right\}, \\ y(t) &= y(0)exp\left\{\int_0^t \left[\tfrac{\delta\lambda x(\xi)}{a+x(\xi)+by(\xi)} - \tfrac{\alpha(\xi)}{1+\beta(\xi)} - m_2\right]\mathrm{d}\xi\right\}, \end{aligned}$$

thus, $x(t) > 0$ and $y(t) > 0$.

From the first formula of the model (3.1), we can get the following inequalities

$$\frac{\mathrm{d}x}{\mathrm{d}t} \le rx(1-\tfrac{x}{K}) - m_1x = x(r-m_1-\tfrac{r}{K}x), \tag{3.2}$$

and according to Lemma 2.1, we discuss the case of $r - m_1$.

If $r - m_1 \leq 0$, then $\dot{x} \leq 0$, so it is clear that $\lim\limits_{t\to\infty} x(t) = 0$. Then, when t is sufficiently large, we can have

$$\frac{\mathrm{d}y}{\mathrm{d}t} \leq \frac{\alpha^U y}{1+\beta y} - m_2 y = \frac{y}{1+\beta y}(\alpha^U - m_2 - m_2\beta y),$$

therefore, the following two situations may occur.

(i) If $\alpha^U - m_2 \leq 0$, then $\dot{y} \leq 0$, then we have $\lim\limits_{t\to\infty} y(t) = 0$.

(ii) If $\alpha^U - m_2 > 0$, then we have $\lim\limits_{t\to\infty} \sup y(t) \leq \frac{\alpha^U - m_2}{m_2\beta}$.

If $r - m_1 > 0$, by applying the Lemma 2.1, we have $\lim\limits_{t\to\infty} \sup x(t) \leq x_{max}$, where x_{max} are positive real roots of equation

$$r - m_1 - \frac{r}{K}x = 0. \tag{3.3}$$

Also, according to $\lim\limits_{t\to\infty} \sup x(t) \leq x_{max}$ and the equation of the model (3.1) we can get

$$\frac{\mathrm{d}y}{\mathrm{d}t} \leq \frac{\delta\lambda x_{max}}{b} + \frac{\alpha^U}{\beta} - m_2 y, \tag{3.4}$$

in the same way, by using Lemma 2.1, the inequality (3.4) signifies that $\lim\limits_{t\to\infty} \sup y(t) \leq y_{max}$, where y_{max} are positive real roots of equation

$$\frac{\delta\lambda x_{max}}{b} + \frac{\alpha^U}{\beta} - m_2 y = 0. \tag{3.5}$$

Solving the Eqs (3.3) and (3.5), we obtain $x_{max} = \frac{(r-m_1)K}{r}$ and $y_{max} = \frac{1}{m_2}(\frac{\delta\lambda x_{max}}{b} + \frac{\alpha^U}{\beta})$. Therefore, we prove that the solution of the model (3.1) is bounded. □

3.2. Possibility of a positive periodic solution

To prove the existence of at least one positive-periodic solution of the model (3.1), we will make use of the following lemmata and definitions.

Lemma 3.1. (Continuation Theorem) [50] Let X and Z be two Banach spaces, $L : \mathrm{Dom}L \subset X \to Z$ be a Fredholm operator with index zero, and $\Omega \subset Z$ be any open bounded set. Also, let $Q : Z \to Z$ be a continuous projection mapping and $N : X \to Z$ be a continuous mapping which is L-compact on Ω. If there exists an isomorphism $J : \mathrm{Im}Q \to \mathrm{Ker}L$ such that

(1) $Lx \neq \lambda Nx$ for every $x \in \partial\Omega \cap \mathrm{Dom}L$ and $\lambda \in (0, 1)$.

(2) $QNx \neq 0$ for every $x \in \partial\Omega \cap \mathrm{Ker}L$.

(3) Let $J : \mathrm{Im}Q \to \mathrm{Ker}L$ be an isomorphism so that the Brouwer degree is $deg\{JQN, \Omega \cap \mathrm{Ker}L\} \neq 0$.

Then, there exists at least one solution to the equation $Lx = Nx$ in $\mathrm{Dom}L \cap \Omega$.

Definition 3.2. [50] Let X and Y be two Banach spaces, and $L : \mathrm{Dom}L \subset X \to Y$ be a linear mapping. If the following conditions are satisfied:

(1) $\mathrm{Im}L$ is a closed subspace of Y.

(2) $dim\mathrm{Ker}L = codim\mathrm{Im}L < \infty$,

then L is called a Fredholm operator with index zero.

Definition 3.3. [50] Let L be a Fredholm operator with index zero. Then there exist linear projection operators $P : X \to \mathrm{Dom}L$, $Q : X \to Y$ such that

(1) ImP = Ker$L$, Ker$Q$ = ImL = Im$(I - Q)$.

(2) X = Ker$L \oplus$ Ker$P$, Y = Im$L \oplus$ ImQ.

The mapping $L_P = L|_{\mathrm{Dom}L \cap \mathrm{Ker}P} : \mathrm{Dom}L \cap \mathrm{Ker}P \to \mathrm{Im}L$ is an invertible mapping. Denote its inverse by K_P, then $K_P : K_P \to \mathrm{Dom}L \cap \mathrm{Ker}P$.

Definition 3.4. [50] Let $L : \mathrm{Dom}L \subset X \to Y$ be a Fredholm operator of index zero, and let $\Omega \subset X$ be an arbitrary open set. Let $N : X \to Y$ be a continuous mapping. If $QN(\bar{\Omega})$ is bounded in Y and $K_P(I - Q)N(\bar{\Omega})$ is a relatively compact set of X, then N is said to be L-compact on Ω.

Definition 3.5. $\phi : \mathrm{Dom}L \cap \mathrm{Ker}L \times [0, 1] \to X$

$$\phi(u, v, \mu) = \begin{pmatrix} r(1 - \frac{e^u}{K})\frac{1}{1+m(t_1)e^v} \\ \frac{\bar{\alpha}}{1+\beta e^v} - m_2 \end{pmatrix} + \mu \begin{pmatrix} -\frac{\lambda e^v}{a+e^u+be^v} - \frac{q_1\bar{e}_1}{c_1e_1(t_2)+c_2e^u} - m_1 \\ \frac{\delta\lambda e^u}{a+e^u+be^v} \end{pmatrix}.$$

In order to simplify the model equations, we assume that $x(t) = e^{u(t)}$, $y(t) = e^{v(t)}$, then the model (3.1) can be written as the following form

$$\begin{cases} \dfrac{\mathrm{d}u(t)}{\mathrm{d}t} = r(1 - \dfrac{e^{u(t)}}{K})\dfrac{1}{1 + m(t)e^{v(t)}} - \dfrac{\lambda e^{v(t)}}{a + e^{u(t)} + be^{v(t)}} - \dfrac{q_1e_1(t)}{c_1e_1(t) + c_2e^{u(t)}} - m_1, \\ \dfrac{\mathrm{d}v(t)}{\mathrm{d}t} = \dfrac{\delta\lambda e^{u(t)}}{a + e^{u(t)} + be^{v(t)}} + \dfrac{\alpha(t)}{1 + \beta e^{v(t)}} - m_2. \end{cases} \tag{3.6}$$

We will consider the model (3.7)

$$\begin{cases} \dfrac{\mathrm{d}u(t)}{\mathrm{d}t} = \lambda U(t, u(t), v(t)), \\ \dfrac{\mathrm{d}v(t)}{\mathrm{d}t} = \lambda V(t, u(t), v(t)), \end{cases} \tag{3.7}$$

where

$$\begin{aligned} U(t, u(t), v(t)) &= r(1 - \tfrac{e^{u(t)}}{K})\tfrac{1}{1+m(t)e^{v(t)}} - \tfrac{\lambda e^{v(t)}}{a+e^{u(t)}+be^{v(t)}} - \tfrac{q_1e_1(t)}{c_1e_1(t)+c_2e^{u(t)}} - m_1, \\ V(t, u(t), v(t)) &= \tfrac{\delta\lambda e^{u(t)}}{a+e^{u(t)}+be^{v(t)}} + \tfrac{\alpha(t)}{1+\beta e^{v(t)}} - m_2. \end{aligned}$$

Lemma 3.2. If $(u(t), v(t))^T$ is a positive ω-periodic solution of the model (3.7), then when the following conditions are met

(1)$0 < m_2 - \delta\lambda < \alpha^U$;

(2)$r > (\frac{\lambda}{b} + \frac{q_1}{c_1} + m_1)(1 + m^U e^{H2})$;

(3)$\alpha^l > m_2$;

there exists a positive number S_1 such that $|u(t)| + |v(t)| \le S_1$, where S_1 is given in the following proof.

Proof. Since $(u(t), v(t))^T$ is a periodic solution of the model (3.7), it suffices to prove that the theorem holds on the interval $[0, \omega]$.

First, let

$$u(\xi_1) = \max_{t\in[0,\omega]} u(t), \quad u(\eta_1) = \min_{t\in[0,\omega]} u(t),$$

$$v(\xi_2) = \max_{t\in[0,\omega]} v(t), \quad v(\eta_2) = \min_{t\in[0,\omega]} v(t),$$

so, we can get

$$\dot{u}(\xi_1) = \dot{u}(\eta_1) = \dot{v}(\xi_2) = \dot{v}(\eta_2) = 0,$$

Substitute $\dot{u}(\xi_1) = \dot{v}(\xi_2) = 0$ into (3.6), and we have

$$\begin{cases} 0 = r(1 - \dfrac{e^{u(\xi_1)}}{K})\dfrac{1}{1 + m(\xi_1)e^{v(\xi 1)}} - \dfrac{\lambda e^{v(\xi_1)}}{a + e^{u(\xi_1)} + be^{v(\xi_1)}} - \dfrac{q_1 e_1(\xi_1)}{c_1 e_1(\xi_1) + c_2 e^{u(\xi_1)}} - m_1, \\ 0 = \dfrac{\delta\lambda e^{u(\xi_2)}}{a + e^{u(\xi_2)} + be^{v(\xi_2)}} + \dfrac{\alpha(\xi_2)}{1 + \beta e^{v(\xi_2)}} - m_2. \end{cases} \tag{3.8}$$

From the first formula of (3.8), we obtain

$$r(1 - \tfrac{e^{u(\xi_1)}}{K})\tfrac{1}{1+m(\xi_1)e^{v(\xi 1)}} = \tfrac{\lambda e^{v(\xi_1)}}{a+e^{u(\xi_1)}+be^{v(\xi_1)}} + \tfrac{q_1 e_1(\xi_1)}{c_1 e_1(\xi_1)+c_2 e^{u(\xi_1)}} + m_1 > 0,$$

further, we get for some H_1,

$$u(t) \le u(\xi_1) \le \ln K := H_1.$$

From the second formula of (3.8), we have

$$m_2 - \delta\lambda - \tfrac{\alpha^U}{1+\beta v(\xi_2)} \le 0,$$

moreover, we get for some H_2,

$$v(t) \le v(\xi_2 \le \ln\left[\tfrac{1}{\beta}(\tfrac{\alpha^U}{m_2-\delta\lambda} - 1)\right] := H_2.$$

Putting $\dot{u}(\eta_1) = \dot{v}(\eta_2) = 0$ into (3.6), we have

$$\begin{cases} 0 = r(1 - \dfrac{e^{u(\eta_1)}}{K})\dfrac{1}{1 + m(\eta_1)e^{v(\eta 1)}} - \dfrac{\lambda e^{v(\eta_1)}}{a + e^{u(\eta_1)} + be^{v(\eta_1)}} - \dfrac{q_1 e_1(\eta_1)}{c_1 e_1(\eta_1) + c_2 e^{u(\eta_1)}} - m_1, \\ 0 = \dfrac{\delta\lambda e^{u(\eta_2)}}{a + e^{u(\eta_2)} + be^{v(\eta_2)}} + \dfrac{\alpha(\eta_2)}{1 + \beta e^{v(\eta_2)}} - m_2. \end{cases} \tag{3.9}$$

From the first formula of (3.9), we can obtain

$$r(1 - \tfrac{e^{u(\eta_1)}}{K})\tfrac{1}{1+m^U e^{H_2}} - \tfrac{\lambda}{b} - \tfrac{q_1}{e_1} - m_1 \le 0,$$

furthermore, we get for some H_3,

$$u(t) \ge u(\eta_1) \ge \ln\left\{\tfrac{K}{r}\left[r - (\tfrac{\lambda}{b} + \tfrac{q_1}{c_1} + m_1)(1 + m^U e^{H_2})\right]\right\} := H_3.$$

From the second formula of (3.9), we obtain

$$\tfrac{\alpha^l}{1+\beta e^{v(\eta_2)}} \le m_2,$$

so, we get for some H_4,

$$v(t) \ge v(\eta_2) \ge \ln\left[\tfrac{1}{\beta}(\tfrac{\alpha^l}{m_2} - 1)\right] := H_4.$$

To sum up, we get

$$H_3 \le u(t) \le H_1, \quad H_4 \le v(t) \le H_2.$$

Let

$$E_1 = \max\{|H_1|, |H_3|\}, \quad E_2 = \max\{|H_2|, |H_4|\}, \quad S_1 = E_1 + E_2,$$

then, we have

$$|u(t)| \le E_1, \quad |v(t)| \le E_2, \quad |u(t)| + |v(t)| \le S_1, \quad \forall t \in [0.\omega].$$

□

If $(u, v)^T$ is a constant vector solution of the model (3.7), then we have

$$\begin{cases} 0 = r(1 - \dfrac{e^u}{K})\dfrac{1}{1 + m(t)e^v} - \dfrac{\lambda e^v}{a + e^u + be^v} - \dfrac{q_1 e_1(t)}{c_1 e_1(t) + c_2 e^u} - m_1, \\ 0 = \dfrac{\delta\lambda e^u}{a + e^u + be^v} + \dfrac{\alpha(t)}{1 + \beta e^v} - m_2. \end{cases} \tag{3.10}$$

Integrating (3.10) on the interval $[0, \omega]$, respectively, and according to the second mean value theorem for integrals, we can obtain

$$\begin{cases} 0 = r(1 - \dfrac{e^u}{K})\dfrac{1}{1 + m(t_1)e^v} - \dfrac{\lambda e^v}{a + e^u + be^v} - \dfrac{q_1 \bar{e}_1}{c_1 e_1(t_2) + c_2 e^u} - m_1, \\ 0 = \dfrac{\delta\lambda e^u}{a + e^u + be^v} + \dfrac{\bar{\alpha}}{1 + \beta e^v} - m_2, \end{cases} \tag{3.11}$$

where, $t_1, t_2 \in [0, \omega]$.

Consider algebraic equations

$$\begin{cases} 0 = r(1 - \dfrac{e^u}{K})\dfrac{1}{1 + m(t_1)e^v} - \mu\left[\dfrac{\lambda e^v}{a + e^u + be^v} + \dfrac{q_1 \bar{e}_1}{c_1 e_1(t_2) + c_2 e^u} + m_1\right], \\ 0 = \mu\dfrac{\delta\lambda e^u}{a + e^u + be^v} + \dfrac{\bar{\alpha}}{1 + \beta e^v} - m_2, \end{cases} \tag{3.12}$$

where, $\mu \in [0, 1]$ is a parameter.

Lemma 3.3. If $(u(t), v(t))^T$ is a solution of the algebraic equations (3.12), then when the following conditions are met

(1) $0 < m_2 - \delta\lambda < \bar{\alpha}$;

(2) $r > (\frac{\lambda}{b} + \frac{q_1 \bar{e}_1}{c_1 e_1^U} + m_1)(1 + m^U e^{G2})$;

(3) $\bar{\alpha} > m_2$;

there exists a positive number S_2 such that $|u| + |v| \le S_2$, where S_2 is given in the following proof.

Proof. From the first formula of (3.12), we obtain

$$r(1 - \tfrac{e^u}{K})\tfrac{1}{1+m(t_1)e^v} = \mu\left[\tfrac{\lambda e^v}{a+e^u+be^v} + \tfrac{q_1 \bar{e}_1}{c_1 e_1(t_2)+c_2 e^u} + m_1\right] > 0,$$

so, we get for some G_1,

$$u < \ln K := G_1.$$

From the second formula of (3.12), we obtain

$$0 \leq \frac{\delta\lambda e^u}{a+e^u+be^v} - m_2 + \frac{\bar{\alpha}}{1+\beta e^v} \leq \delta\lambda - m_2 + \frac{\bar{\alpha}}{1+\beta e^v},$$

so, we get for some G_2,

$$v < \ln\left[\frac{1}{\beta}(\frac{\bar{\alpha}}{m_2-\delta\lambda} - 1)\right] := G_2.$$

From the first formula of (3.12) and G_2, we have

$$0 \geq r(1-\frac{e^u}{K})\frac{1}{1+m(t_1)e^{G_2}} - \frac{\lambda}{b} - \frac{q_1\bar{e}_1}{c_1e_1^U} - m_1,$$

then, we get for some G_3,

$$u \geq \ln\left\{\frac{K}{r}\left[r - (\frac{\lambda}{b} + \frac{q_1\bar{e}_1}{c_1e_1^v} + m_1)(1 + m^U e^{G_2})\right]\right\} := G_3.$$

From the second formula of (3.12), we have

$$m_2 - \frac{\bar{\alpha}}{1+\beta e^v} > 0,$$

moreover, we get for some G_4,

$$v > \ln\left[\frac{1}{\beta}(\frac{\bar{\alpha}}{m_2} - 1)\right] := G_4.$$

Combining the above inequalities, we can obtain

$$G_3 \leq u \leq G_1, \quad G_4 \leq v \leq G_2.$$

Let

$$E_3 = \max\{|G_1|, |G_3|\}, \quad E_4 = \max\{|G_2|, |G_4|\}, \quad S_2 = E_3 + E_4,$$

then, we have

$$|u| \leq E_3, \quad |v| \leq E_4, \quad |u| + |v| \leq S_2.$$

□

Theorem 3.2. If the conditions of Lemmata 3.2 and 3.3 are satisfied, then, the model (3.1) has at least one positive ω-periodic solution.

Proof. Assume that $x(t) = e^{u(t)}$, $y(t) = e^{v(t)}$, then the model (3.1) can be written as the model (3.6).

Define

$$X = Y = \left\{z(t) = (u(t), v(t))^T \in C(R, R^2) | z(t+\omega) = z(t)\right\},$$
$$\|z(t)\| = \left\|(u(t), v(t))^T\right\| = \max_{t\in[0,\omega]}|u(t)| + \max_{t\in[0,\omega]}|v(t)|,$$

then, X and Y together with the norm $\|\cdot\|$, are both Banach spaces.

For $z(t) \in X$, the operator is defined as follows

$$L : \mathrm{Dom}L \cap X \to Y, \quad Lz = \frac{\mathrm{d}z}{\mathrm{d}t}, \quad Pz = z(0), Qz = \frac{1}{\omega}\int_0^\omega z(t)dt, \quad N : X \to Y,$$
$$Nz = \begin{pmatrix} rx(1-\frac{x}{K})\frac{1}{1+m(t)y} - \frac{\lambda xy}{a+x+by} - \frac{q_1e_1(t)x}{c_1e_1(t)+c_2x} - m_1x \\ \frac{\delta\lambda xy}{a+x+by} + \frac{\alpha(t)y}{1+\beta y} - m_2y \end{pmatrix},$$

so that, we have

$$\mathrm{Ker}L = \{z(t) \in X | Lz = 0\}, \quad \mathrm{Im}L = \left\{z(t) \in Y | \int_0^\omega z(t)dt = 0\right\}, \quad dim\mathrm{Ker}L = codim\mathrm{Im}L = 2.$$

According to the Lebesgue dominated convergence theorem, it can be proved that ImL is closed in Y. Therefore, L is a Fredholm operator with index zero.

Obviously, both P and Q are continuous projection operators and satisfy

$$\mathrm{Im}P = \mathrm{Ker}L, \quad \mathrm{Im}L = \mathrm{Ker}Q = \mathrm{Im}(I-Q), \quad X = \mathrm{Ker}L \oplus \mathrm{Ker}P, \quad Y = \mathrm{Im}L \oplus \mathrm{Im}Q,$$

which means that L is invertible on Dom$L \cap$ Ker$P$, and its inverse is $K_P : \mathrm{Im}L \to \mathrm{Dom}L \cap \mathrm{Ker}P$, which is denoted as

$$K_P(z) = \int_0^t z(s)ds - \tfrac{1}{\omega}\int_0^\omega dt \int_0^t z(s)ds.$$

For all $z(t) \in X$, we have

$$QNz = Q(F_1(t,u(t),v(t)), F_2(t,u(t),v(t)))^T = (\tfrac{1}{\omega}\int_0^\omega F_1(t,u(t),v(t))dt, \tfrac{1}{\omega}\int_0^\omega F_2(t,u(t),v(t))dt)^T = (\bar{F}_1, \bar{F}_2)^T.$$

Let

$$\varphi_i(t) = \int_0^t F_i(s,u(s),v(s))ds + (\tfrac{2}{\omega} - t)\bar{F}_i - \tfrac{1}{\omega}\int_0^\omega dt \int_0^t F_i(s,u(s),v(s))ds, \quad i = 1,2,$$

then

$$K_P(I-Q)Nz = (\varphi_1(t), \varphi_2(t))^T.$$

Therefore, according to the Lebesgue dominated convergence theorem, we get both QN and $K_P(I-Q)N$ are continuous.

Suppose that

$$\Omega = \left\{ z(t) = (u(t), v(t))^T \in X \,|\, \|z(t)\| \le S \right\},$$

where

$$S = S_1 + S_2 + \varepsilon, \quad \varepsilon > 0.$$

Since $F_i(t,u(t),v(t))$ is bounded within $[0,\omega] \times \bar{\Omega}$, $QN(\bar{\Omega})$ and $K_P(I-Q)N(\bar{\Omega})$ is uniformly bounded and equally continuous within $[0,\omega]$. According to the Arzela-Ascoli theorem, both $QN(\bar{\Omega})$ and $K_P(I-Q)N(\bar{\Omega})$ are compact sets. Therefore, N is L-compact on $\bar{\Omega}$.

Subsequently, we proceed to validate the three conditions of the continuation theorem respectively.

(1) For every $z(t) \in \partial\Omega \cap \mathrm{Dom}L$ and $\lambda \in (0,1)$, $Lz \neq \lambda Nz$

Using proof by contradiction, if $Lz = \lambda Nz$, then $z(t)$ is a positive ω-periodic solution of the model (3.6). Then, according to Lemma 3.3, we have $\|z(t)\| \le S_1$. However, since $z(t) \in \partial\Omega \cap \mathrm{Dom}L$, $\|z(t)\| = S$, which contradicts the conclusion mentioned above. Therefore, we have verified the first condition of the continuation theorem.

(2) $QNx \neq 0$ for every $x \in \partial\Omega \cap \mathrm{Ker}L$

Using proof by contradiction again, if $QNz = 0$, then $z = (u,v)^T$ is a solution of (3.12), when $\mu = 1$. So, $\|z\| \le S_2$, which contradicts $\|z\| = S > S_2$. Therefore, we have verified the second condition of the continuation theorem.

(3) $deg\{JQN, \Omega \cap \mathrm{Ker}L\} \neq 0$

For all $z(t) \in \mathrm{Im}Q$, we obtain $Jz = z$, hence, $z(t) \in \Omega \cap \mathrm{Ker}L$, $z = (u,v)^T$ is a constant vector. Therefore,

$$\begin{aligned} JQN(u,v)^T &= JQ(F_1(t,u,v), F_2(t,u,v))^T \\ &= (\frac{1}{\omega}\int_0^\omega F_1(t,u,v)dt, \frac{1}{\omega}\int_0^\omega F_2(t,u,v)dt)^T \end{aligned}$$

$$= \begin{pmatrix} r(1-\frac{e^u}{K})\frac{1}{1+m(t_1)e^v} - \frac{\lambda e^v}{a+e^u+be^v} - \frac{q_1\bar{e}_1}{c_1e_1(t_2)+c_2e^u} - m_1 \\ \frac{\delta\lambda e^u}{a+e^u+be^v} + \frac{\bar{\alpha}}{1+\beta e^v} - m_2 \end{pmatrix},$$

and $JQN(u,v)^T = \phi(u,v,1)$, where $(u,v)^T \in \partial\Omega \cap \mathrm{Ker}L$, $\phi(u,v,1) \neq (0,0)^T$. Otherwise, $(u,v)^T$ is a solution of (3.12), and $\left\|(u,v)^T\right\| \leq S_2$ contradicts $(u,v)^T \in \partial\Omega \cap \mathrm{Ker}L$. Then, according to the homotopy invariance of the topological degree, we can obtain

$$\begin{aligned} deg\left\{JQN(u,v,\mu), \mathrm{Ker}L\cap\Omega, (0,0)^T\right\} &= deg\left\{\phi(u,v,1), \mathrm{Ker}L\cap\Omega, (0,0)^T\right\} \\ &= deg\left\{\phi(u,v,0), \mathrm{Ker}L\cap\Omega, (0,0)^T\right\} \\ &= deg\left\{(r(1-\frac{e^u}{K})\frac{1}{1+m(t_1)e^v}, \frac{\bar{\alpha}}{1+\beta e^v} - m_2)^T, \mathrm{Ker}L\cap\Omega, (0,0)^T\right\}. \end{aligned}$$

Consider the algebraic equation

$$\begin{cases} r(1-\dfrac{e^u}{K})\dfrac{1}{1+m(t_1)e^v} = 0, \\ \dfrac{\bar{\alpha}}{1+\beta e^v} - m_2 = 0. \end{cases} \tag{3.13}$$

From (3.13), we get

$$v^* = \ln\left[\tfrac{1}{\beta}(\tfrac{\bar{\alpha}}{m_2} - 1)\right], \quad u^* = \ln\left[K - \tfrac{K(1+m(t_1)e^{v^*})}{r}\right],$$

where $(u^*, v^*)^T \in \mathrm{Ker}L \cap \Omega$ is the unique solution of (3.13). Let

$$\psi_1(u,v) = r(1-\tfrac{e^u}{K})\tfrac{1}{1+m(t_1)e^v}, \quad \psi_2(u,v) = \tfrac{\bar{\alpha}}{1+\beta e^v} - m_2,$$

so we have

$$\tfrac{\partial\psi_1}{\partial u} = -\tfrac{r}{K}\tfrac{e^u}{1+m(t_1)e^v}, \quad \tfrac{\partial\psi_1}{\partial v} = -r(1-\tfrac{e^u}{K})\tfrac{m(t_1)e^v}{(1+m(t_1)e^v)^2}, \quad \tfrac{\partial\psi_2}{\partial u} = 0, \quad \tfrac{\partial\psi_2}{\partial v} = -\tfrac{\bar{\alpha}\beta e^v}{(1+\beta e^v)^2},$$

then

$$\begin{aligned} deg\left\{JQN(u,v)^T, \mathrm{Ker}L\cap\Omega, (0,0)^T\right\} &= sgn\begin{vmatrix} \frac{\partial\psi_1(u,v)}{\partial u} & \frac{\partial\psi_1(u,v)}{\partial v} \\ \frac{\partial\psi_2(u,v)}{\partial u} & \frac{\partial\psi_2(u,v)}{\partial v} \end{vmatrix}_{(u^*,v^*)} \\ &= sgn\begin{vmatrix} -\frac{r}{K}\frac{e^{u^*}}{1+m(t_1)e^{v^*}} & -r(1-\frac{e^{u^*}}{K})\frac{m(t_1)e^{v^*}}{(1+m(t_1)e^{v^*})^2} \\ 0 & -\frac{\bar{\alpha}\beta e^{v^*}}{(1+\beta e^{v^*})^2} \end{vmatrix} \\ &= sgn\left\{\frac{r\bar{\alpha}\beta e^{u^*}e^{v^*}}{K(1+m(t_1)e^{v^*})(1+\beta e^{v^*})^2}\right\} = 1 \neq 0. \end{aligned}$$

Consequently, we have successfully verified the third condition of Lemma 3.1. From this, we know that the model (3.1) has at least one ω-periodic positive solution within the intersection of Ω and Dom$L$, which is denoted as $(u,v)^T$. It is easy to derive that $x(t) = e^u(t)$ and $y(t) = e^v(t)$. Therefore, we can conclude that $(u(t), v(t))$ constitutes an ω-periodic solution of the nonautonomous model (3.1). □

3.3. The global attractiveness of the positive periodic solution

Lemma 3.4. [50] Consider a real number n, and let f denote a nonnegative and integrable function that exhibits uniform continuity defined over the interval $[n, \infty)$. In such a case, it follows that as t approaches positive infinity, the limit of $f(t)$ tends to zero.

Definition 3.6. $(\bar{x}(t), \bar{y}(t))^T$ is a positive ω-periodic solution of (3.1), and $(x(t), y(t))^T$ is an arbitrary positive solution of the model (3.1). If $(\bar{x}(t), \bar{y}(t))^T$ and $(x(t), y(t))^T$ satisfies

$$\lim_{t\to\infty} |x(t) - \bar{x}(t)| = 0, \quad \lim_{t\to\infty} |y(t) - \bar{y}(t)| = 0,$$

then $(\bar{x}(t), \bar{y}(t))^T$ is globally attractive.

Theorem 3.3. Assume that the solutions of the model (3.1) remain bounded. If Σ_1 and Σ_2 satisfy the following conditions

(1) $\Sigma_1 = \mu_1 \left[\frac{rm^l}{(1+m^U L_2)^2} - \frac{rm^U L_1}{K(1+m^l K_2)^2} + \frac{\lambda(a+K_1)}{(a+L_1+bL_2)^2} \right] - \mu_2 \left[\frac{\delta\lambda b L_1}{a+K_1+bK_2} + \frac{\alpha^U \beta}{(1+\beta K_2)^2} \right] > 0;$

(2) $\Sigma_2 = \mu_1 \left[\frac{\frac{r}{K}}{1+m^U K_2} - \frac{\lambda L_2}{(a+K_1+bK_2)^2} - \frac{q_1 e_1^U c_2}{(c_1 e_1^l + c_2 K_1)^2} \right] - \mu_2 \frac{\delta\lambda(a+bL_2)}{(a+K_1+bK_2)^2} > 0;$

then the model (3.1) will have a positively ω- periodic solution with global attractiveness.

Proof. Because the model (3.1) has at least one positive ω-periodic solution $(\bar{x}(t), \bar{y}(t))^T$, we get

$$e^{H_3} \le \bar{x}(t) \le e^{H_1}, \quad e^{H_4} \le \bar{y}(t) \le e^{H_2},$$

moreover, due to the solution of the model (3.1) being bounded, we let

$$K_1 \le x(t), \bar{x}(t) \le L_1, \quad K_2 \le y(t), \bar{y}(t) \le L_2.$$

We define a Lyapunov function as

$$V(t) = V_1(t) + V_2(t),$$

where

$$V_1(t) = \mu_1 \left| \ln x(t) - \ln \bar{x}(t) \right|, \quad V_2(t) = \mu_2 \left| \ln y(t) - \ln \bar{y}(t) \right|.$$

Take the right upper derivatives of $V_1(t)$ and $V_2(t)$, respectively, we can obtain

$$\begin{aligned}
D^+V_1(t) &= \mu_1 sgn(x(t) - \bar{x}(t))\left(\frac{\dot{x}(t)}{x(t)} - \frac{\dot{\bar{x}}(t)}{\bar{x}(t)}\right) \\
&\le \mu_1 \left[-\frac{rm(t)}{(1+m(t)y)(1+m(t)\bar{y})} + \frac{rm(t)\bar{x}}{K(1+m(t)y)(1+m(t)\bar{y})} - \frac{\lambda(x+a)}{(a+x+by)(a+x+b\bar{y})} \right] |y(t) - \bar{y}(t)| \\
&+ \mu_1 \left[-\frac{r}{K(1+m(t)y)} + \frac{\lambda\bar{y}}{(a+x+by)(a+x+b\bar{y})} + \frac{q_1 e_1(t) c_2}{(c_1 e_1(t) + c_2 x)(c_1 e_1(t) + c_2 \bar{x})} \right] |x(t) - \bar{x}(t)| \\
&\le \mu_1 \left[-\frac{rm^l}{(1+m^U L_2)^2} + \frac{rm^U L_1}{K(1+m^l K_2)^2} - \frac{\lambda(K_1+a)}{(a+L_1+bL_2)^2} \right] |y(t) - \bar{y}(t)| \\
&+ \mu_1 \left[-\frac{r}{K(1+m^U L_2)} + \frac{\lambda L_2}{(a+K_1+bK_2)^2} + \frac{q_1 e_1^U c_2}{(c_1 e_1^l + c_2 K_1)^2} \right] |x(t) - \bar{x}(t)|,
\end{aligned}$$

$$
\begin{aligned}
D^+V_2(t) &= \mu_1 sgn(y(t)-\bar{y}(t))\left(\frac{\dot{y}(t)}{y(t)}-\frac{\dot{\bar{y}}(t)}{\bar{y}(t)}\right)\\
&\le \mu_2\left[\frac{\delta\lambda b\bar{x}}{(a+x+by)(a+\bar{x}+b\bar{y})}+\frac{\alpha(t)\beta}{(1+\beta y)(1+\beta\bar{y})}\right]|y(t)-\bar{y}(t)|\\
&+\mu_2\frac{\delta\lambda(a+b\bar{y})}{(a+x+by)(a+\bar{x}+b\bar{y})}|x(t)-\bar{x}(t)|\\
&\le \mu_2\left[\frac{\delta\lambda bL_1}{(a+K_1+bK_2)^2}+\frac{\alpha^U\beta}{(1+\beta K_2)^2}\right]|y(t)-\bar{y}(t)|+\mu_2\frac{\delta\lambda(a+bL_2)}{(a+K_1+bK_2)^2}|x(t)-\bar{x}(t)|.
\end{aligned}
$$

Based on the above two equations, we can have

$$
\begin{aligned}
D^+V(t) &= D^+V_1(t)+D^+V_2(t)\\
&\le |y(t)-\bar{y}(t)|\left\{\mu_1\left[-\frac{rm^l}{(1+m^UL_2)^2}+\frac{rm^UL_1}{K(1+m^lK_2)^2}-\frac{\lambda(K_1+a)}{(a+L_1+bL_2)^2}\right]\right.\\
&\left.+\mu_2\left[\frac{\delta\lambda bL_1}{(a+K_1+bK_2)^2}+\frac{\alpha^U\beta}{(1+\beta K_2)^2}\right]\right\}+|x(t)-\bar{x}(t)|\left\{\mu_1\left[-\frac{r}{K(1+m^UL_2)}+\frac{\lambda L_2}{(a+K_1+bK_2)^2}\right.\right.\\
&\left.\left.+\frac{q_1e_1^Uc_2}{(c_1e_1^l+c_2K_1)^2}\right]+\mu_2\frac{\delta\lambda(a+bL_2)}{(a+K_1+bK_2)^2}\right\}\\
&\le -|y(t)-\bar{y}(t)|\left\{\mu_1\left[\frac{rm^l}{(1+m^UL_2)^2}-\frac{rm^UL_1}{K(1+m^lK_2)^2}+\frac{\lambda(K_1+a)}{(a+L_1+bL_2)^2}\right]\right.\\
&\left.-\mu_2\left[\frac{\delta\lambda bL_1}{(a+K_1+bK_2)^2}+\frac{\alpha^U\beta}{(1+\beta K_2)^2}\right]\right\}-|x(t)-\bar{x}(t)|\left\{\mu_1\left[\frac{r}{K(1+m^UL_2)}-\frac{\lambda L_2}{(a+K_1+bK_2)^2}\right.\right.\\
&\left.\left.-\frac{q_1e_1^Uc_2}{(c_1e_1^l+c_2K_1)^2}\right]-\mu_2\frac{\delta\lambda(a+bL_2)}{(a+K_1+bK_2)^2}\right\}.
\end{aligned}
$$

Let

$$
\begin{aligned}
\Sigma_1 &= \mu_1\left[\tfrac{rm^l}{(1+m^UL_2)^2}-\tfrac{rm^UL_1}{K(1+m^lK_2)^2}+\tfrac{\lambda(a+K_1)}{(a+L_1+bL_2)^2}\right]-\mu_2\left[\tfrac{\delta\lambda bL_1}{a+K_1+bK_2}+\tfrac{\alpha^U\beta}{(1+\beta K_2)^2}\right]>0,\\
\Sigma_2 &= \mu_1\left[\tfrac{\frac{r}{K}}{1+m^UK_2}-\tfrac{\lambda L_2}{(a+K_1+bK_2)^2}-\tfrac{q_1e_1^Uc_2}{(c_1e_1^l+c_2K_1)^2}\right]-\mu_2\tfrac{\delta\lambda(a+bL_2)}{(a+K_1+bK_2)^2}>0.
\end{aligned}
$$

Then we have

$$
D^+V(t) = -\Sigma_1|y(t)-\bar{y}(t)|-\Sigma_2|x(t)-\bar{x}(t)|,
$$

integrate the above expression from T to t and simplify it briefly, where $t>T>0$, then we obtain

$$
V(t)+\Sigma_1\int_T^t|y(s)-\bar{y}(s)|\,ds+\Sigma_2\int_T^t|x(s)-\bar{x}(s)|\,ds\le V(T).
$$

Therefore, we get that the solution of the model (3.1) is bounded. Consequently, the derivative of the solution is bounded and $|x(s)-\bar{x}(s)|$, $|y(s)-\bar{y}(s)|$ are uniformly continuous. According to Lemma 3.4, we can obtain

$$
\lim_{t\to\infty}|x(t)-\bar{x}(t)|=0,\quad \lim_{t\to\infty}|y(t)-\bar{y}(t)|=0.
$$

In this way, we have proved that the positive periodic solution $(\bar{x}(t),\bar{y}(t))^T$ of the model (3.1) is globally attractive.

Next, we will prove that this solution is unique. We consider $(\bar{x}_1(t), \bar{y}_1(t))^T$ and $(\bar{x}_2(t), \bar{y}_2(t))^T$, which are positive ω-periodic solutions different from the model (3.1) and are globally attractive. Therefore, there exists $\xi \in [0, \omega]$, such that $\bar{x}_1(\xi) \neq \bar{x}_2(\xi)$. There also exists $\varepsilon > 0$, such that

$$\varepsilon = |\bar{x}_1(\xi) - \bar{x}_2(\xi)| = \lim_{n\to\infty} |\bar{x}_1(\xi + n\omega) - \bar{x}_2(\xi + n\omega)| = \lim_{t\to\infty} |\bar{x}_1(t) - \bar{x}_2(t)| > 0.$$

This contradicts the fact that the solution is globally attractive. Hence, we have $\bar{x}_1(t) = \bar{x}_2(t)$ and $\bar{y}_1(t) = \bar{y}_2(t)$, and we have proved that the model (3.1) has a unique positive ω-periodic solution which is globally attractive. □

Regarding nonautonomous predator-prey model (3.1), we introduced some ecological environmental factors with seasonal periodicity, which not only can make the ecological dynamic relationship represented by the predator-prey model closer to the actual dynamic relationship in the field, but also can induce the predator-prey model to have specific dynamic states, which can represent the population persistent survival. Mathematical theory mainly investigated the boundedness of solution, possibility of positive periodic solution, and global attractiveness of positively ω-periodic solution. These results directly indicated that some key parameters with seasonal periodic disturbances could induce predator and prey to form the periodic oscillatory growth coexistence, which indirectly proved that nonautonomous predator-prey model can more accurately represent the periodic survival status in the wild than the autonomous predator-prey model.

4. Numerical simulation analysis

4.1. Numerical results for the autonomous model (1.2)

In order to verify the effectiveness and feasibility of the theoretical derivation work, and visualize the evolution process of specific bifurcation dynamics behavior, we conduct relevant bifurcation dynamics evolution simulations on the model (1.2) with different growth coefficients α values with the help of Matlab software.

4.1.1. Numerical results for transcritical bifurcation

When we take the values of other parameters according to Table 2, we can directly compute $\alpha_{TC} = 0.142329$. The model (1.2) exhibits two boundary equilibrium points E_{23} and E_{24}. When $\alpha = 0.14 < \alpha_{TC}$, the boundary equilibrium point E_{23} is an unstable saddle point, whereas the boundary equilibrium point E_{24} is a stable node (seeing Figure 3(a)). When $\alpha = 0.142329 = \alpha_{TC}$, the boundary equilibrium point E_{24} transforms into a saddle-node point, while the boundary equilibrium point E_{23} remains a saddle point (seeing Figure 3(b)). Furthermore, when $\alpha = 0.15 > \alpha_{TC}$, the boundary equilibrium point E_{24} becomes a saddle point (seeing Figure 3(c)). This implies that as α value increases, the stability of the boundary equilibrium point E_{24} shifts from stable to unstable, which implies that predator populations will not gradually go extinct.

4.1.2. Numerical results for saddle-node bifurcation

When we take the values of other parameters according to Table 2, we can easily compute $\alpha_{SN} = 0.222761$. This implies that as α value varies around α_{SN}, the number of the internal equilibrium point in the model (1.2) changes from 0 to 2. It is easy to find from Figure 4 that when $\alpha = 0.23 > \alpha_{SN} =$

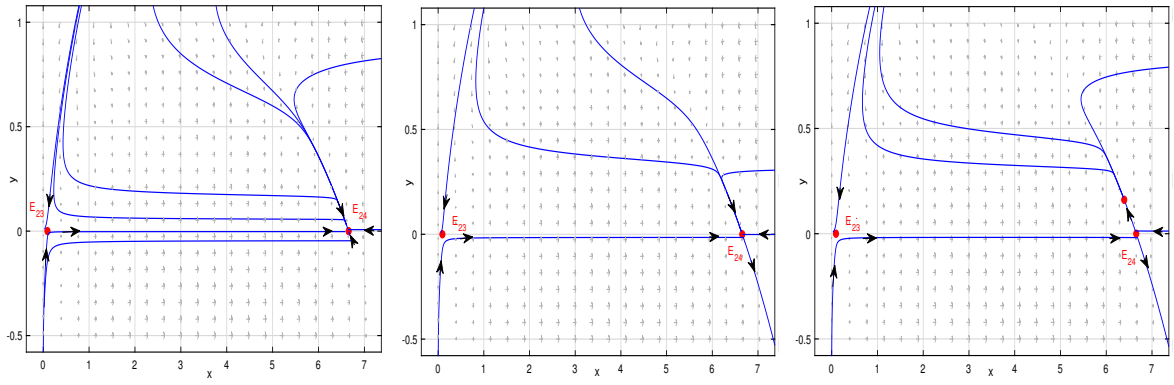

(a) $\alpha = 0.14$ (b) $\alpha = 0.142329$ (c) $\alpha = 0.15$

Figure 3. The process of transcritical bifurcation according to the bifurcation parameter α, and the values of other parameters are from Table 2. (a) saddle E_{23} and stable node E_{24}; (b) saddle E_{23} and saddle-node E_{24}; (c) saddle E_{23} and saddle E_{24}.

0.222761, the model (1.2) has no internal equilibrium point, when $\alpha = 0.222761$; the model (1.2) has an internal equilibrium point E_+, which is a saddle-node point; when $\alpha = 0.2227$, the model (1.2) has two internal equilibrium points E_1^* and E_2^*, where E_1^* is a saddle point and E_2^* is an unstable node. These research results not only directly indicate that predator and prey can form a transient constant growth coexistence mode, but also suggest that the model (1.2) will exhibit more diverse dynamic behaviors.

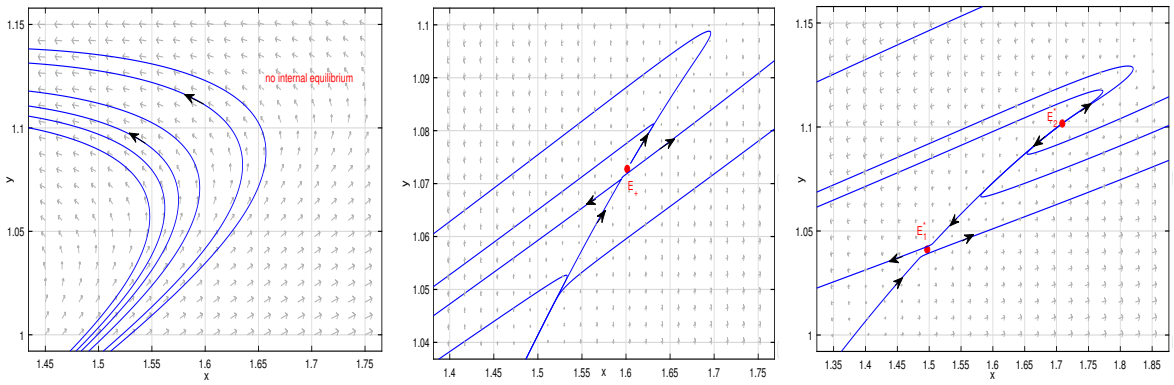

(a) $\alpha = 0.23$ (b) $\alpha = 0.222761$ (c) $\alpha = 0.2227$

Figure 4. The process of saddle-node bifurcation according to the bifurcation parameter α, and the values of other parameters are from Table 2. (a) no internal equilibrium point; (b) a unique internal equilibrium point E_+; (c) two internal equilibrium points E_1^* and E_2^*.

4.1.3. Numerical results for Hopf bifurcation

When we take the values of other parameters according to Table 2, we can easily calculate $\alpha_H = 0.220689$, which implies that as α value varies around α_H, the model (1.2) will generate stable or unstable limit cycles. Additionally, the first Lyapunov number is $l_1 = -0.3719835444 < 0$, indicating that this limit cycle is stable. In Figure 5(a), when $\alpha = 0.222 > \alpha_H$, the model (1.2) has an unstable

focus E_2^*. As α value decreases to 0.220689, the unstable focus transforms into a center in Figure 5(b), marking the critical state of the model (1.2). Further, when $\alpha = 0.2205 < \alpha_H$, the center becomes a stable focus in Figure 5(d), and the model (1.2) produces a stable limit cycle in Figure 5(c). These research results directly indicate that predator and prey can form a steady state periodic oscillation growth coexistence mode, which means that predator and prey can grow and coexist for a long time within a certain range.

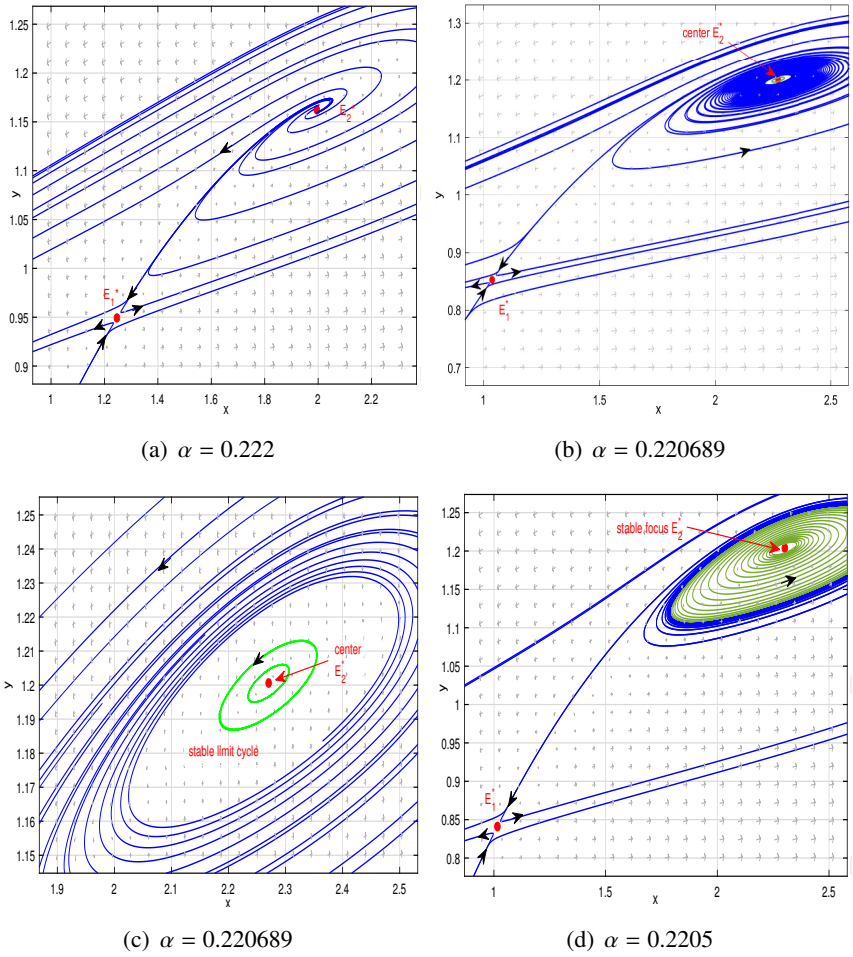

(a) $\alpha = 0.222$ (b) $\alpha = 0.220689$

(c) $\alpha = 0.220689$ (d) $\alpha = 0.2205$

Figure 5. The process of Hopf bifurcation according to the bifurcation parameter α, and the values of other parameters are from Table 2. (a) unstable focus E_2^*; (b) E_2^* is a center; (c) partial amplification with $(x, y) \in [1.9, 2.5] \times [1.15, 1.25]$ for (b), and a stable periodic orbits around E_2^*; (d) a stable focus E_2^*.

4.1.4. Numerical results for Bogdanov-Takens bifurcation

When we take the values of other parameters according to Table 3, we can calculate the Bogdanov-Takens bifurcation critical values $\alpha_{BT} = 0.272888$ and $\lambda_{BT} = 0.419147$. The numerical simulation results are shown in Figure 6, which can reveal the complex dynamical behaviors of the model (1.2) near the critical points. When the values of key parameters α and λ vary slightly around the critical values $(\alpha_{BT}, \lambda_{BT})$, the dynamical behaviors of the model (1.2) change essentially, and the population

growth coexistence modes also exhibit significant dynamic variations.

Table 3. Parameter values.

r	K	m	a	b	q_1	e_1	c_1	c_2	m_1	δ	β	m_2
0.8	10	0.2	3	0.1	0.25	0.3	0.4	0.25	0.2	0.15	0.3	0.2

The synergistic effect of the Beddington-DeAngelis functional response parameter λ and the Smith growth parameter α can induce the Bogdanov-Takens bifurcation phenomenon, which can significantly influence the population growth coexistence modes. Specifically:

(i) When the coefficients satisfy $(\varepsilon_1, \varepsilon_2) = (0, 0)$, as is shown in Figure 6(a), the model (2.16) exhibits a codimension-two cusp.

(ii) As the perturbations ε_1 and ε_2 decrease to $(0.01, -0.0015)$, the model (2.16) has no equilibrium points, as is shown in Figure 6(b).

(iii) Further decreasing ε_1 and ε_2 to $(0.01, -0.002033)$, the model (2.16) has an unstable saddle point and an unstable focus, as is shown in Figure 6(c).

(iv) When $(\varepsilon_1, \varepsilon_2) = (0.01, -0.002046)$, an unstable limit cycle rotates around a center and a saddle point, as is shown in Figure 6(d).

(v) As ε_1 and ε_2 decrease to $(0.01, -0.002059)$, the model (2.16) has a stable focus enclosed by an unstable homoclinic orbit and a saddle point, as is shown in Figure 6(e).

(vi) Finally, when $(\varepsilon_1, \varepsilon_2) = (0.01, -0.00207)$, as is shown in Figure 6(f), the model (2.16) has a saddle point and a stable focus.

This numerical simulation result not only verifies the correctness and feasibility of the theorem, but also reveals that minor perturbations ε_1 and ε_2 in the parameter space of α and λ can trigger drastic transitions in the ecological model's states, which may manifest as constant steady state growth coexistence mode or periodic oscillatory growth coexistence mode.

4.2. Numerical results for the nonautonomous model

To verify the correctness and feasibility of the Theorems 3.1, 3.2 and 3.3, we conducted numerical simulations on periodic solutions of the nonautonomous model (3.1) with the help of Matlab software. Meanwhile, it is worth noting that although the some parameters in ecological models might naturally exhibit diverse periods, for the sake of computational convenience, we standardized all parameter periods to 90 days. Moreover, it must be admitted that changing the periods of these periodic functions could lead to different results, which highlights the model's sensitivity to temporal dynamics. In the model (3.1), we set

$$\alpha(t) = \alpha + \alpha_{11} sin(\omega t), \quad e_1(t) = e_1 + e_{11} sin(\omega t), \quad m(t) = m + m_{11} sin(\omega t),$$

and we adopt the following parameter value set in Table 4. It is obvious that the model (3.1) is unstable at this point.

First, while we keep other parameters unchanged, we consider the seasonal variation of the predator's Smith growth parameter, while the prey harvesting parameter and fear effect parameter will remain aseasonal (i.e., $e_{11} = 0, m_{11} = 0$). When $\alpha_{11} = 0.1$, the model (3.1) can exhibit a single periodic solution (seen in Figure 7(a)). At the same time, we plotted phase portraits of the model (3.1)

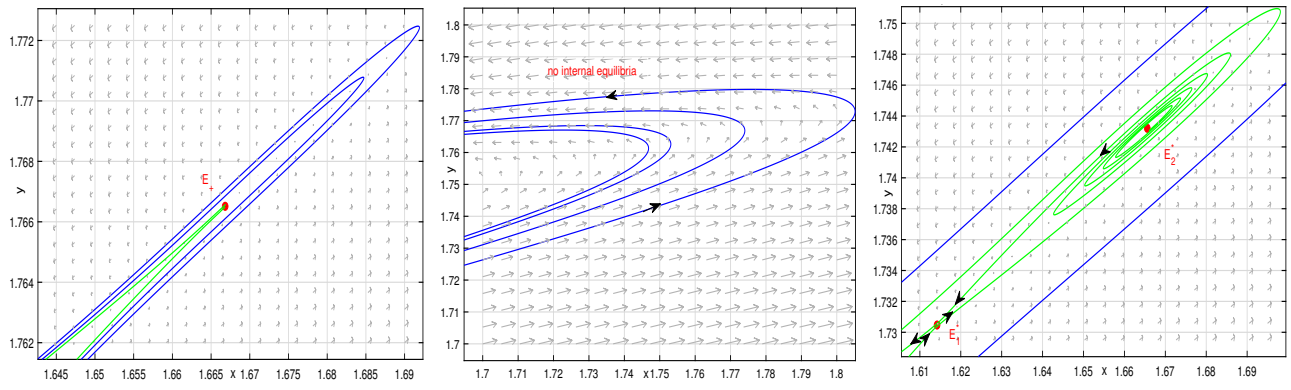

(a) $(\varepsilon_1, \varepsilon_2) = (0, 0)$ (b) $(\varepsilon_1, \varepsilon_2) = (0.01, -0.0015)$ (c) $(\varepsilon_1, \varepsilon_2) = (0.01, -0.002033)$

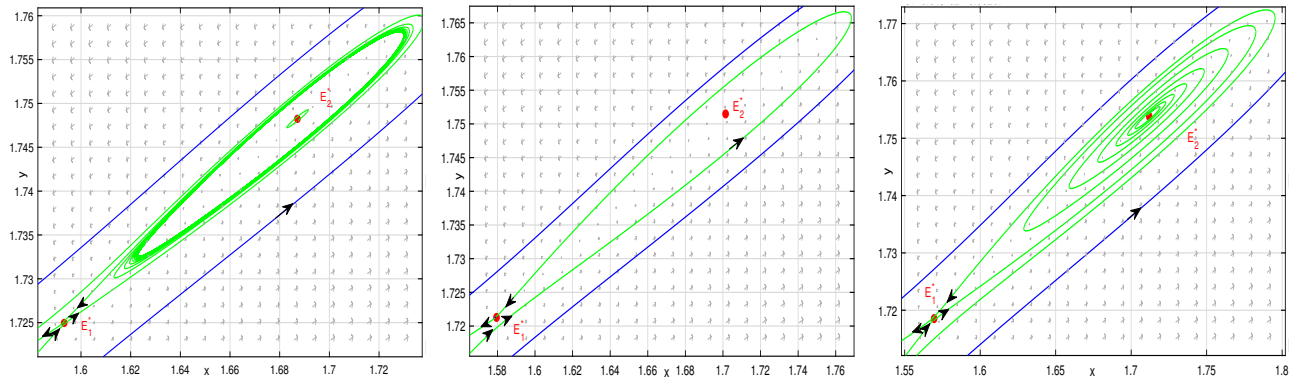

(d) $(\varepsilon_1, \varepsilon_2) = (0.01, -0.002046)$ (e) $(\varepsilon_1, \varepsilon_2) = (0.01, -0.002059)$ (f) $(\varepsilon_1, \varepsilon_2) = (0.01, -0.00207)$

Figure 6. $\alpha_{BT} = 0.272888$, $\lambda_{BT} = 0.419147$ and the values of other parameters are from Table 3. The dynamic evolution process of B-T bifurcation of the model (2.16). (a) A cusp with codimension 2 when $(\varepsilon_1, \varepsilon_2) = (0, 0)$; (b) no equilibrium point when $(\varepsilon_1, \varepsilon_2) = (0.01, -0.0015)$; (c) unstable saddle and an unstable focus when $(\varepsilon_1, \varepsilon_2) = (0.01, -0.002033)$; (d) There exists a stable focus surrounded by an unstable limit cycle and a saddle when $(\varepsilon_1, \varepsilon_2) = (0.01, -0.002046)$; (e) There exists a stable focus surrounded by an unstable homoclinic orbit and a saddle when $(\varepsilon_1, \varepsilon_2) = (0.01, -0.002059)$; (f) There exist a saddle and a stable focus when $(\varepsilon_1, \varepsilon_2) = (0.01, -0.00207)$.

Table 4. Parameter values.

r	K	m	a	b	q_1	e_1	c_1	c_2	m_1	δ	β	m_2	α	λ
0.9	10	0.2	2	0.5	0.1	0.4	0.4	0.1	0.1	0.1	0.35	0.13	0.18	0.1

under five different initial values: $(8.2, 1.5)$, $(8.1, 1.3)$, $(8.4, 1.4)$, $(8, 1.3475)$ and $(8.5, 1.348)$, as is shown in Figure 7(b). It is obvious that solution trajectories from different initial conditions can ultimately converge to the periodic solution, which can confirm that this single periodic solution is globally stable. Thus, this research result can directly indicate that the periodic per-capita reproduction rate can induce predator and prey to form a steady state periodic oscillation growth coexistence mode.

Second, we discuss the seasonal variation of the prey harvesting parameter, while the per-capita

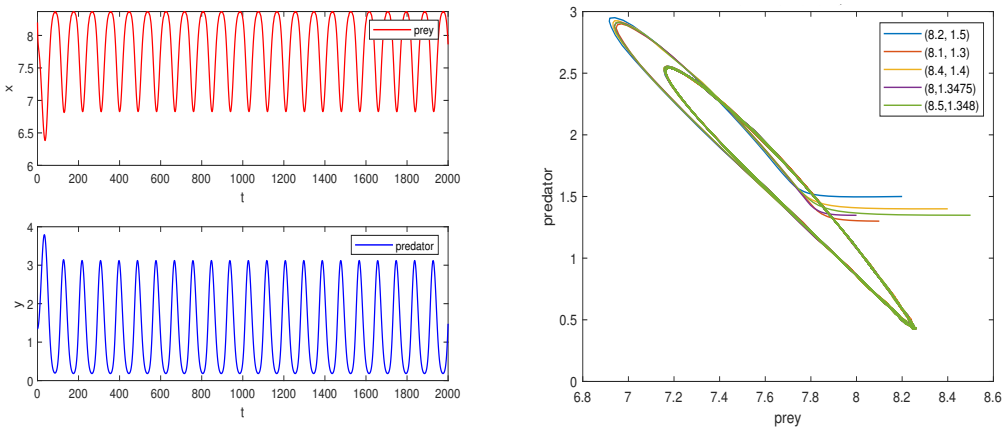

(a) (b)

Figure 7. (a) solution time series of the model (3.1) for $\alpha_{11} = 0.1$; (b) Phase portraits of the model (3.1) with five different initial values $(8.2, 1.5)$, $(8.1, 1.3)$, $(8.4, 1.4)$, $(8, 1.3475)$, $(8.5, 1.348)$. Solution trajectories stemming from diverse initial conditions can ultimately converge to a single periodic solution. The values of other parameters are from Table 4.

reproduction rate parameter and fear effect parameter will remain aseasonal (i.e., $\alpha_{11} = 0, m_{11} = 0$). When $e_{11} = 0.2$, the model (3.1) possesses a simple periodic solution (seen in Figure 8(a)). Furthermore, we construct phase portraits of the model (3.1) under five distinct initial values: $(8.2, 1.347)$, $(8.1, 1.347)$, $(8.4, 1.348)$, $(8, 1.3475)$ and $(8.5, 1.348)$. Thus, it is easy to find from Figure 8(b) that solution trajectories originating from different initial conditions can eventually converge to this single periodic solution, which can confirm that this single periodic solution is globally stable. This research result can directly indicate that the prey periodic harvest amount can induce predator and prey to form a steady state periodic oscillation growth coexistence mode.

Finally, we address the seasonal variation of the prey's fear effect parameter, while the per-capita reproduction rate parameter and prey harvesting parameter will remain aseasonal (i.e., $\alpha_{11} = 0, e_{11} = 0$). When $m_{11} = 0.05$, the model (3.1) harbors a simple periodic solution (seen in Figure 9(a)). Meanwhile, we generate phase portraits of the model(3.1) under five diverse initial values: $(7.95, 1.34)$, $(7.95, 1.342)$, $(7.9, 1.343)$, $(7.7, 1.341)$ and $(7.8, 1.342)$. It is obvious to find from Figure 9(b) that solution trajectories emanating from distinct initial conditions will ultimately converge to the simple periodic solution, which can confirm that this single periodic solution is globally stable. This research result can directly indicate that the periodic fear effect can induce predator and prey to form a steady state periodic oscillation growth coexistence mode.

By comparing the numerical simulation results of the model (1.2) and model (3.1), it can be concluded from Figures 3–6 that the model (1.2) has rich bifurcation dynamics, which can drive predator and prey to form steady state constant growth coexistence mode and steady state periodic oscillation growth coexistence mode. Meanwhile, it is even more worth emphasizing from Figures 7–9 that the model (3.1) has stable periodic solutions when the key parameter values are subject to seasonal periodic disturbances, which indicates that predator and prey have a stable periodic oscillation growth coexistence mode. Although both the model (1.2) and model (3.1) have a

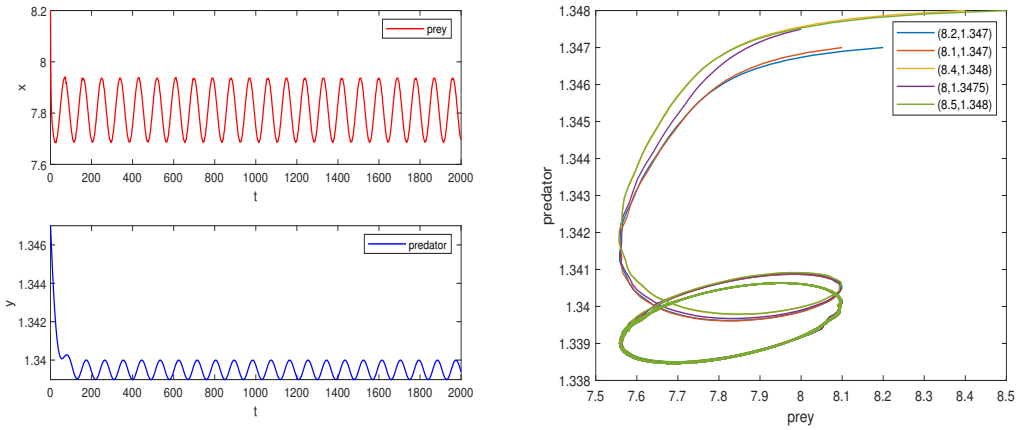

(a) (b)

Figure 8. (a) solution time series of the model (3.1) for $e_{11} = 0.2$; (b) Phase portraits of the model (3.1) with five different initial values $(8.2, 1.347)$, $(8.1, 1.347)$, $(8.4, 1.348)$, $(8, 1.3475)$, $(8.5, 1.348)$. Solution trajectories stemming from diverse initial conditions ultimately converge to a single periodic solution. The values of other parameters are from Table 4.

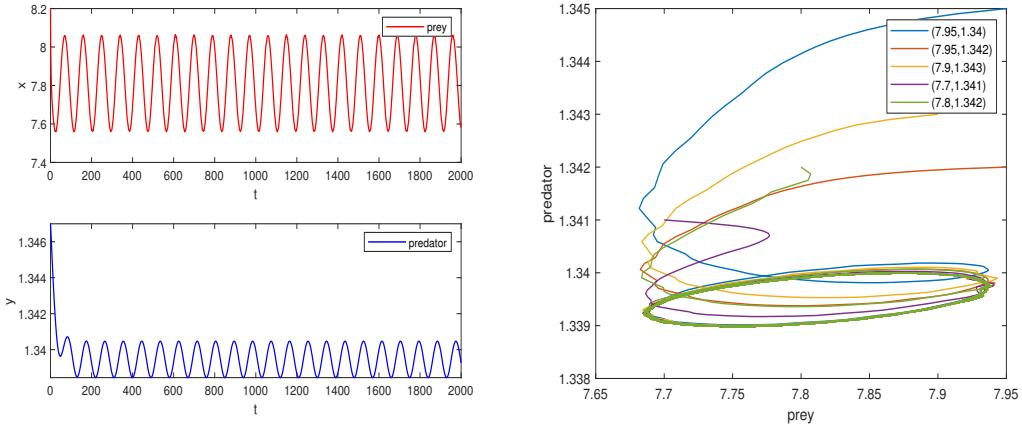

(a) (b)

Figure 9. (a) solution time series of the model (3.1) for $m_{11} = 0.05$; (b) Phase portraits of the model (3.1) with five different initial values $(7.95, 1.34)$, $(7.95, 1.342)$, $(7.9, 1.343)$, $(7.7, 1.341)$, $(7.8, 1.342)$. Solution trajectories stemming from diverse initial conditions ultimately converge to a single periodic solution. The values of other parameters are from Table 4.

steady state periodic oscillation persistent survival state, the model (3.4) is induced by seasonal periodic disturbances, which is more in line with the natural laws of the field. Therefore, relatively speaking, the model (3.1) is more suitable for application in field data monitoring.

5. Conclusions

In the paper, on the one hand, an autonomous predator-prey model with nonlinear harvesting and Beddington-DeAngelis functional response was proposed to explore the specific bifurcation dynamics and population growth coexistence mode both theoretically and numerically. Mathematical theoretical work not only has investigated the dissipation and persistence of the model (1.2) as well as the existence and local stability of all equilibrium points, but also derived the threshold conditions for the model (1.2) to exhibit transcritical bifurcation, saddle-node bifurcation, Hopf bifurcation, and Bogdanov-Takens bifurcation. These research results were both the theoretical basis for subsequent numerical simulations and the triggering mechanism for the formation of some growth coexistence modes between predator and prey. The numerical simulation work not only verified the correctness and feasibility of the theoretical derivation results, but also dynamically displayed the evolution process of specific bifurcation dynamics behaviors. Thus, it was worth emphasizing from Figures 3–5 that as the per-capita reproduction α values changed, the bifurcation dynamics of the model (1.2) would undergo a fundamental change, which suggested that the evolutionary state of predator population has gone through a gradual extinction state, a constant steady state existence state, and a steady state periodic oscillation existence state, and the evolutionary state of prey population has gone through a gradual extinction state or a gradual maximum survival state, a constant steady state existence state, and a steady state periodic oscillation existence state. Meanwhile, it also needed to be pointed out from Figure 6 that when the values of per-capita reproduction α and the maximum predation rate λ would undergo slight changes simultaneously, the growth coexistence model of predator and prey could switch back and forth between constant steady state and steady state periodic oscillation.

On the other hand, we introduced the seasonal cyclical effects of some key ecological environmental factors, and constructed a nonautonomous predator-prey model with nonlinear harvesting and Beddington-DeAngelis functional response. The existence and attractiveness of positive ω periodic solutions in the model (3.1) were theoretically analyzed in detail, which indicated that periodic perturbations of key parameters could induce the formation of the steady state periodic oscillation growth coexistence mode between predator and prey. At the same time, it was clearly known from Figures 7–9 that periodic perturbations of the prey's fear effect, the per-capita reproduction rate and prey harvesting could all drive the model (3.1) to have attractive positive periodic solutions, which indicated that the seasonal cyclical effects of ecological environmental factors could induce the formation of periodic oscillation growth coexistence mode in populations.

One innovation of this paper was the introduction of fear effect and nonlinear harvesting for prey population in the modeling process, which not only could enhance the predator-prey model (1.2) as more controllable and complex, but also could make it more suitable for exploring the dynamic evolution trends of wild predatory ecosystems. Another innovation of this paper was the proposal of a nonautonomous predator-prey model (3.1) to explore the impact of some key parameters with time periodic disturbances, The research results indicated that time periodic disturbances could promote the model (3.1) to have stable periodic solutions. Furthermore, it was worth emphasizing that the level of fear effect, the harvest amount of prey population and the per-capita reproduction rate with seasonal periodic disturbance could respectively lead to the formation of stable periodic oscillatory growth coexistence mode between prey and predator.

In summary, the research findings of this paper indicated that the values of some key ecological environmental factors could promote the formation of different growth coexistence modes in populations, and periodic disturbances of some key ecological environmental factors could induce the formation of periodic oscillation growth coexistence modes in populations. Finally, it was our hope that these results would contribute to the rapid development of research on the dynamic behaviors of predator-prey ecological models.

Acknowledgments

This research was supported by the Science and Technology Major Program of Wenzhou, China (Grant No.ZS2022005), Zhejiang Province College Students' Science and Technology Innovation Activity Plan (New Talent Plan) (Grant No. 2025R444A017 and 2024R429A010), and Wenzhou University National College Students Innovation and Entrepreneurship Training Plan Project (Grant No. JWXC 2024081).

Conflict of interest

The authors declare there is no conflict of interest.

References

1. A. J. Lotka, Elements of physical biology, *Nature*, **16** (1925), 461. https://doi.org/10.1038/116461b0
2. V. Volterra, Fluctuations in the abundance of a species considered mathematically, *Nature*, **118** (1926), 558–560. https://doi.org/10.1038/118558a0
3. A. Korobeinikov, A Lyapunov function for Leslie-Gower predator-prey models, *Appl. Math. Lett.*, **14** (2001), 697–699. https://doi.org/10.1016/S0893-9659(01)80029-X
4. P. H. Leslie, A stochastic model for studying the properties of certain biological systems by numerical methods, *Biometrika*, **45** (1958), 16–31. https://doi.org/10.2307/2333042
5. A. Erbach, F. Lutscher, G. Seo, Bistability and limit cycles in generalist predator–prey dynamics, *Ecol. Complexity*, **14** (2013), 48–55. https://doi.org/10.1016/j.ecocom.2013.02.005
6. G. Mandal, L. N. Guin, S. Chakravarty, Dynamical inquest of refuge and bubbling issues in an interacting species system, *Commun. Nonlinear Sci. Numer. Simul.*, **129** (2024), 107700. https://doi.org/10.1016/j.cnsns.2023.107700
7. B. Mondal, S. Sarkar, U. Ghosh, Complex dynamics of a generalist predator–prey model with hunting cooperation in predator, *Eur. Phys. J. Plus*, **137** (2022), 43. https://doi.org/10.1140/epjp/s13360-021-02272-4
8. Y. L. Cai, C. D. Zhao, W. M. Wang, J. F. Wang, Dynamics of a Leslie-Gower predator-prey model with additive Allee effect, *Appl. Math. Modell.*, **39** (2015), 2092–2106. https://doi.org/10.1016/j.apm.2014.09.038

9. D. Sen, S. Ghorai, S. Sharma, M. Banerjee, Allee effect in prey's growth reduces the dynamical complexity in prey-predator model with generalist predator, *Appl. Math. Modell.*, **91** (2021), 768–790. https://doi.org/10.1016/j.apm.2020.09.046

10. J. W. Jia, D. P. Hu, R. K. Upadhyay, Z. W. Zheng, N. N. Zhu, M. Liu, Canard cycle, relaxation oscillation and cross-diffusion induced pattern formation in a slow-fast ecological system with weak Allee effect, *Commun. Nonlinear Sci. Numer. Simul.*, **140** (2025), 108360. https://doi.org/10.1016/j.cnsns.2024.108360

11. Z. C. Shang, Y. H. Qiao, Multiple bifurcations in a predator-prey system of modified Holling and Leslie type with double Allee effect and nonlinear harvesting, *Math. Comput. Simul.*, **205** (2023), 745–764. https://doi.org/10.1016/j.matcom.2022.10.028

12. X. Wang, L. Zanette, X. Zou, Modelling the fear effect in predator-prey interactions, *J. Math. Biol.*, **73** (2016), 1179–1204. https://doi.org/10.1007/s00285-016-0989-1

13. X. Wang, X. Zou, Modeling the fear effect in predator-prey interactions with adaptive avoidance of predators, *Bull. Math. Biol.*, **79** (2017), 1325–1359. https://doi.org/10.1007/s11538-017-0287-0

14. M. M. Chen, Y. Takeuchi, J. F. Zhang, Dynamic complexity of a modified Leslie-Gower predator-prey system with fear effect, *Commun. Nonlinear Sci. Numer. Simul.*, **119** (2023), 107109. https://doi.org/10.1016/j.cnsns.2023.107109

15. S. Creel, D. Christianson, Relationships between direct predation and risk effects, *Trends Ecol. Evol.*, **23** (2008), 194–201. http://dx.doi.org/10.1016/j.tree.2007.12.004

16. S. L. Lima, L. M. Dill, Behavioral decisions made under the risk of predation: A review and prospectus, *Can. J. Zool.*, **68** (1990), 619–640. https://doi.org/10.1139/z90-092

17. J. R. Beddington, Mutual interference between parasites or predators and its effect on searching efficiency, *J. Anim. Ecolo.*, **44** (1975), 331–340. https://doi.org/10.2307/3866

18. X. Z. Feng, C. Sun, W. B. Yang, C. T. Li, Dynamics of a predator-prey model with nonlinear growth rate and B-D functional response, *Nonlinear Anal. Real World Appl.*, **70** (2023), 103766. https://doi.org/10.1016/j.nonrwa.2022.103766

19. R. P. Gupta, P. Chandra, Bifurcation analysis of modified Leslie-Gower predator-prey model with Michaelis–Menten type prey harvesting, *J. Math. Anal. Appl.*, **398** (2013), 278–295. https://doi.org/10.1016/j.jmaa.2012.08.057

20. F. D. Chen, Y. M. Chen, Z. Li, L. J. Chen, Note on the persistence and stability property of a commensalism model with Michaelis-Menten harvesting and Holling type II commensalistic benefit, *Appl. Math. Lett.*, **134** (2022), 108381. https://doi.org/10.1016/j.aml.2022.108381

21. D. P. Hu, H. J. Cao, Stability and bifurcation analysis in a predator-prey system with Michaelis-Menten type predator harvesting, *Nonlinear Anal. Real World Appl.*, **33** (2017), 58–82. https://doi.org/10.1016/j.nonrwa.2016.05.010

22. D. P. Hu, L. Y. Ma, Z. G. Song, Z. W. Zheng, L. F. Cheng, M. Liu, Multiple bifurcations of a time-delayed coupled FitzHugh-Rinzel neuron system with chemical and electrical couplings, *Chaos Solitons Fractals*, **180** (2024), 114546. https://doi.org/10.1016/j.chaos.2024.114546

23. X. B. Zhang, Q. An, A. Moussaoui, Effect of density-dependent diffusion on a diffusive predator-prey model in spatially heterogeneous environment, *Math. Comput. Simul.*, **227** (2025), 1–18. https://doi.org/10.1016/j.matcom.2024.07.022

24. L. L. Ding, X. B. Zhang, G. Y. Lv, Dynamics of a plankton community with delay and herd-taxis, *Chaos Solitons Fractals*, **184** (2024), 114974. https://doi.org/10.1016/j.chaos.2024.114974

25. B. Mondal, S. Mandal, P. K. Tiwari, R. K. Upadhyay, How predator harvesting affects prey-predator dynamics in deterministic and stochastic environments, *Appl. Math. Comput.*, **498** (2025), 129380. https://doi.org/10.1016/j.amc.2025.129380

26. Y. Tian, J. Zhu, J. Zheng, K. B. Sun, Modeling and analysis of a prey-predator system with prey habitat selection in an environment subject to stochastic disturbances, *Electron. Res. Arch.*, **33**(2025), 744–767. https://doi.org/10.3934/era.2025034

27. Y. Tian, H. Guo, W. Y. Shen, X. R. Yan, J. Zheng, K. B. Sun, Dynamic analysis and validation of a prey-predator model based on fish harvesting and discontinuous prey refuge effect in uncertain environments, *Electron. Res. Arch.*, **33** (2025), 973–994. https://doi.org/10.3934/era.2025044

28. X. R. Yan, Y. Tian, K. B. Sun, Hybrid effects of cooperative hunting and inner fear on the dynamics of a fishery model with additional food supplement, *Math. Methods Appl. Sci.*, **48** (2025), 9389–9403. https://doi.org/10.1002/mma.10805

29. M. Ch-Chaoui, K. Mokni, A discrete evolutionary Beverton-Holt population model, *Int. J. Dyn. Control*, **11** (2023), 1060–1075. https://doi.org/10.1007/s40435-022-01035-y

30. M. Ch-Chaoui, K. Mokni, A multi-parameter bifurcation analysis of a prey-predator model incorporating the prey Allee effect and predator-induced fear, *Nonlinear Dyn.*, **113** (2025), 18879–18911. https://doi.org/10.1007/s11071-025-11063-w

31. K. Mokni, S. Elaydi, M. Ch-Chaoui, A. Eladdaoi, Discrete evolutionary population models: A new approach, *J. Biol. Dyn.*, **14** (2020), 454–478. https://doi.org/10.1080/17513758.2020.1772997

32. B. X. Li, L. H. Zhu, Turing instability analysis of a reaction-diffusion system for rumor propagation in continuous space and complex networks, *Inf. Process. Manage.*, **61** (2024), 103621. https://doi.org/10.1016/j.ipm.2023.103621

33. H. Y. Sha, L. H. Zhu, Dynamic analysis of pattern and optimal control research of rumor propagation model on different networks, *Inf. Process. Manage.*, **62** (2025), 104016. https://doi.org/10.1016/j.ipm.2024.104016

34. J.Y. Shi, L. H. Zhu, Turing pattern theory on homogeneous and heterogeneous higher-order temporal network system, *J. Math. Phys.*, **66** (2025), 042706. https://doi.org/10.1063/5.0211728

35. L. H. Zhu, Y. Ding, S. L. Shen, Green behavior propagation analysis based on statistical theory and intelligent algorithm in data-driven environment, *Math. Biosci.*, **379** (2025), 109340. https://doi.org/10.1016/j.mbs.2024.109340

36. T. Y. Yuan, G. Guan, S. L. Shen, L. H. Zhu, Stability analysis and optimal control of epidemic-like transmission model with nonlinear inhibition mechanism and time delay in both homogeneous and heterogeneous networks, *J. Math. Anal. Appl.*, **526** (2023), 127273. https://doi.org/10.1016/j.jmaa.2023.127273

37. G. W. He, F. D. Chen, L. Zhong, L. J. Chen, The influence of saturated fear effects on species dynamics: A Lotka-Volterra competition model analysis, *Int. J. Biomath.*, **23** (2025),2550037. https://doi.org/10.1142/S1793524525500378

38. A. K. Umrao, S. Roy, P. K. Tiwari, P. K. Srivastava, Dynamical behaviors of autonomous and nonautonomous models of generalist predator-prey system with fear, mutual interference and nonlinear harvesting, *Chaos Solitons Fractals*, **183** (2024), 114891. https://doi.org/10.1016/j.chaos.2024.114891

39. D. Barman, S. Roy, P. K. Tiwari, S. Alam, Two fold impacts of fear in a seasonally forced predator-prey system with Cosner functional response, *J. Biol. Syst.*, **31** (2023), 517–555. DOI:10.1142/S0218339023500183

40. A. L. Greggor, J. W. Jolles, A. Thornton, N. S. Clayton, Seasonal changes in neophobia and its consistency in rooks: The effect of novelty type and dominance position, *Anim. Behav.*, **121** (2013), 11–20. http://dx.doi.org/10.1016/j.anbehav.2016.08.010

41. K. H. Elliott, G. S. Betini, I. Dworkin, D. R. Norris, Experimental evidence for withinand cross-seasonal effects of fear on survival and reproduction, *J. Anim. Ecol.*, **85** (2016), 507–515. http://dx.doi.org/10.1111/1365-2656.12487.

42. S. Y. Tang, R. A. Cheke, Y. N. Xiao, Optimal impulsive harvesting on non-autonomous Beverton-Holt difference equations, *Nonlinear Anal. Theory*, **65** (2006), 2311–2341. https://doi.org/10.1016/j.na.2006.02.049

43. X. M. Feng, Y. F. Liu, S. G. Ruan, J. S. Yu, Periodic dynamics of a single species model with seasonal Michaelis-Menten type harvesting, *J. Differ. Equations*, **354** (2023), 237–263. https://doi.org/10.1016/j.jde.2023.01.014

44. Y. F. Liu, X. M. Feng, S. G. Ruan, J. S. Yu, Periodic dynamics of a single species model with seasonal Michaelis-Menten type harvesting, II: Existence of two periodic solutions, *J. Differ. Equations*, **388** (2024), 253–282. https://doi.org/10.1016/j.jde.2024.01.004

45. S. Roy, P. K. Tiwari, Bistability in a predator-prey model characterized by the Crowley-Martin functional response: Effects of fear, hunting cooperation, additional foods and nonlinear harvesting, *Math. Comput. Simul.*, **228** (2025), 274–297. https://doi.org/10.1016/j.matcom.2024.09.001

46. Z. F. Zhang, T. R. Ding, W. Z. Huang, Z. X. Dong, *Qualitative Theory of Differential Equation*, Science Press, 1992.

47. L. Perko, *Differential Equations and Dynamical Systems*, Springer, 2001. https://doi.org/10.1007/978-1-4613-0003-8

48. J. Chen, J. C. Huang, S. G. Ruan, J. H. Wang, Bifurcations of invariant tori in predatorprey models with seasonal prey harvesting, *SIAM J. Appl. Math.*, **73** (2013), 1876–1905. https://doi.org/10.1137/120895858

49. J. C. Huang, Y. J. Gong, J. Chen, Multiple bifurcation in a predator-prey system of Holling and Leslie type with constant-yield prey harvesting, *Int. J. Bifurcation Chaos*, **23** (2013), 1350164. https://doi.org/10.1142/S0218127413501642

50. R. E. Gaines, J. L. Mawhin, *Coincidence Degree and Nonlinear Differential Equations*, Springer, 2006. https://doi.org/10.1007/BFb0089537

AIMS Press